

Supplementary Material for ‘Ice sheet flow with thermally activated sliding. Part 1: The role of advection’

Elisa Mantelli^{1,2,*}, Marianne Haseloff^{2,**}, Christian Schoof²

¹Geophysics Department, Stanford University, Stanford (CA), USA

²Department of Earth, Ocean and Atmospheric Sciences, University of British
Columbia, Vancouver, CA

*present address: AOS Program, Princeton University, Princeton (NJ), USA

**present address: Department of Earth Sciences, University of Oxford, Oxford,
UK

October 8, 2019

Contents

1	Supporting information for §2	3
1.1	Master model	3
1.2	Non-dimensionalization	4
2	Supporting information for §3	6
2.1	Outer problem	6
2.2	Boundary layer model	7
2.3	The velocity field near the onset	9
2.4	The strong advection limit, $Pe_{BL} \gg 1$	10
2.5	The advection-diffusion boundary layer on the cold side	10
2.6	The advection-diffusion boundary layer near the origin, $ X \leq Pe_{BL}^{-2/3}$	13
2.7	The advection-diffusion boundary layer on the temperate side	15
2.8	Numerical solution of the ice thickness scale problem	17
3	Supporting information for §4	25
3.1	Freezing in the subtemperate region with $\delta \sim O(1)$	25
4	Supporting information for §5	26
4.1	Model reformulation in a stretched coordinate system	26
4.2	Discretization	29
4.3	Numerical solution of the steady state problem	34
4.4	A discontinuous acceleration at the subtemperate - temperate boundary	34

5	The length of the subtemperate region with $Pe = 0$	36
5.1	On Fowler's (2001) argument about the impossibility of a hard switch	36
5.2	A constraint from energy conservation	37

1 Supporting information for §2

1.1 Master model

Consider the flow of a two dimensional ice sheet as governed by the Stokes equations

$$\frac{\partial \tau_{ij}}{\partial x_j} - \frac{\partial p}{\partial x_i} + \rho g_i = 0, \quad (1a)$$

where τ_{ij} is the deviatoric part of the stress tensor $\sigma_{ij} = \tau_{ij} - p\delta_{ij}$, p is pressure, ρ is the density of the ice, and g_i is the component of gravity in the i direction. We assume a Cartesian coordinate system $(x_1, x_2) = (x, z)$ such that the z -axis is vertical and oriented upward, with $z = 0$ at sea level, as well as the summation convention. Deviatoric stresses are related to the strain rate tensor D_{ij} through

$$\tau_{ij} = 2\eta D_{ij}, \quad \text{with} \quad D_{ij} = \frac{1}{2} \left(\frac{\partial u_i}{\partial x_j} + \frac{\partial u_j}{\partial x_i} \right), \quad (1b)$$

with the velocity field $\mathbf{u} = (u_1, u_2) = (u, w)$ satisfying incompressibility

$$\nabla \cdot \mathbf{u} = 0, \quad (1c)$$

and $\nabla = (\partial/\partial x, \partial/\partial z)$. In eq. (1b) η is the viscosity, which we regard as constant. Disregarding the dependence of viscosity on temperature and strain rate implies that we rule out any thermo-mechanical feedback, consistently with our objective to investigate the role of basal thermal transitions with respect to fast flow initiation in isolation.

Let us assume that the upper surface of the ice in contact with the atmosphere is $z = s(x, t)$, and the lower surface in contact with the bed is $z = b(x)$, so that the ice has thickness $h(x, t) = s - b$, and let \mathbf{n}_i , $\hat{\mathbf{n}}_i$ be upward-pointing vectors normal to the surface and to the bed, respectively. The surface is stress-free and also a free boundary, that is

$$\sigma_{ij}n_j = 0, \quad \text{and} \quad \frac{\partial s}{\partial t} + u \frac{\partial s}{\partial x} - w = \dot{b} \quad \text{on} \quad z = s, \quad (1d)$$

with

$$\mathbf{n} = \left(-\frac{\partial s}{\partial x}, 1 \right) / \sqrt{1 + \left(\frac{\partial s}{\partial x} \right)^2}, \quad (1e)$$

where \dot{b} is the rate of snow accumulation per unit area if $\dot{b} > 0$, or mass loss through sublimation or melting if $\dot{b} < 0$. The bed is a material surface where there may or may not be slip: here we are concerned with the case of thermally controlled sliding, so we associate a frozen bed with no slip and a thawed bed with basal sliding. In the former case we have

$$\mathbf{u} = 0 \quad \text{on} \quad z = b \quad \text{if} \quad T < T_m, \quad (1f)$$

where $T(x, z, t)$ is temperature and T_m is the melting point temperature, which we consider independent of pressure. If slip occurs, we assume that there is an applied shear stress τ_b at the base of the ice sheet that is a function of the basal velocity u_b through a linear slip law [1, 2]

$$\tau_b = C u_b, \quad \mathbf{u} \cdot \hat{\mathbf{n}} = 0 \quad \text{on} \quad z = b \quad \text{if} \quad T = T_m, \quad (1g)$$

where $C > 0$ denotes the friction coefficient. Defining the normal vector to the bed as

$$\hat{\mathbf{n}} = \left(-\frac{\partial b}{\partial x}, 1 \right) / \sqrt{1 + \left(\frac{\partial b}{\partial x} \right)^2} \quad (1h)$$

sliding velocity and basal shear stress are

$$u_b = u \left[1 + \left(\frac{\partial b}{\partial x} \right)^2 \right]^{1/2}, \quad \tau_b = \frac{\left[1 - \left(\frac{\partial b}{\partial x} \right)^2 \right] \tau_{xz} - 2 \frac{\partial b}{\partial x} \tau_{xx}}{1 + \left(\frac{\partial b}{\partial x} \right)^2}. \quad (1i)$$

Even with a viscosity independent of temperature, we require a thermal model to know whether the bed is frozen or thawed. Energy conservation for the ice and the bed reads

$$\rho c \left(\frac{\partial T}{\partial t} + \mathbf{u} \cdot \nabla T \right) - \nabla \cdot (\kappa \nabla T) = \tau_{ij} D_{ij} \quad \text{for } b < z < s, \quad (2a)$$

$$\rho_{bed} c_{bed} \frac{\partial T}{\partial t} - \nabla \cdot (\kappa_{bed} \nabla T) = 0 \quad \text{for } z < b, \quad (2b)$$

where c is heat capacity, κ is the thermal conductivity, and the subscript *bed* denotes the physical properties of the bed. We prescribe a temperature T_{surf} at the surface, and a geothermal heat flux q_{geo} at large distance below the ice-bed contact,

$$T = T_S \quad \text{on } z = s, \quad (2c)$$

$$- \kappa_{bed} \frac{\partial T}{\partial z} \rightarrow q_{geo} \quad \text{as } z \rightarrow -\infty, \quad (2d)$$

while at the bed $z = b$ we require

$$\kappa \frac{\partial T}{\partial z} \Big|_{z \rightarrow b^+} - \kappa_{bed} \frac{\partial T}{\partial z} \Big|_{z \rightarrow b^-} = [T]_-^+ = 0 \quad \text{if } T < T_m, \quad (2e)$$

or

$$T = T_m \quad \text{if } u_b > 0, \quad (2f)$$

where $[f(z)]_-^+ = f(z \rightarrow z_0^+) - f(z \rightarrow z_0^-)$ denotes the difference between positive and negative limiting values of f across a prescribed surface $z = z_0$.

1.2 Non-dimensionalization

We consider scales for the ice sheet length $[x] = L$, surface accumulation $[\dot{b}]$, temperature $[T] = [T_s] - T_m$ as known quantities, and introduce the usual, shallow ice scale relationships [e.g., 3]

$$[w] = [\dot{b}], \quad [u] = \frac{[w][x]}{[z]}, \quad [t] = \frac{[x]}{[u]}, \quad [p] = \rho g [z], \quad [\tau] = \frac{\rho g [z]^2}{[x]}, \quad [z] = \left(\frac{\eta [\dot{b}] [x]^2}{\rho g} \right)^{1/4}, \quad (3a)$$

in addition to the non-dimensional parameters

$$Pe = \frac{[z]^2}{\lambda [t]}, \quad \alpha = \frac{[\tau][u]}{\kappa [T]/[z]}, \quad \gamma = C \frac{[u]}{[\tau]}, \quad \nu = \frac{q_{geo}[z]}{\kappa [T]}, \quad \varepsilon = \frac{[z]}{[x]}, \quad (3b)$$

where Pe is the Péclet number, α is the strength of strain heating compared to the background conductive heat flux, γ is a non-dimensional friction coefficient, ν is a non-dimensional geothermal heat flux, ε is the aspect ratio of the ice sheet, and $\lambda = \kappa(\rho c)^{-1}$ is the thermal diffusivity of the ice. From this point onward we assume that ice and bed have the same physical properties, so we drop the subscript *bed*.

Equipped with these scales, we rescale model variables as

$$x = [x]x^*, \quad z = [z]z^*, \quad t = [t]t^*, \quad s(x, t) = [z]s^*(x^*, t^*), \quad b(x) = [z]b^*(x^*), \quad (3c)$$

$$u = [u]u^*, \quad w = [w]w^*, \quad \dot{b} = [\dot{b}]\dot{b}^*, \quad p = \rho g[z](s^* - z^*) + \varepsilon[\tau]p^*, \quad (3d)$$

$$\tau_{xz} = [\tau]\tau_{xz}^*, \quad \tau_{xx} = -\tau_{zz} = \varepsilon[\tau]\tau_{xx}^* = -\varepsilon[\tau]\tau_{zz}^*, \quad T = [T]T^* + T_m, \quad (3e)$$

Dropping stars for simplicity the full, non-dimensional mass and momentum conservation read

$$\frac{\partial u}{\partial x} + \frac{\partial w}{\partial z} = 0, \quad (4a)$$

$$\varepsilon^2 \frac{\partial \tau_{xx}}{\partial x} + \frac{\partial \tau_{xz}}{\partial z} - \varepsilon p_x - \frac{\partial s}{\partial x} = 0, \quad (4b)$$

$$\varepsilon^2 \left(\frac{\partial \tau_{zx}}{\partial x} + \frac{\partial \tau_{zz}}{\partial z} \right) - \varepsilon \frac{\partial p}{\partial z} = 0, \quad (4c)$$

with the constitutive relationships given by

$$\tau_{xx} = 2 \frac{\partial u}{\partial x}, \quad \tau_{zz} = 2 \frac{\partial w}{\partial z}, \quad \tau_{xz} = \tau_{zx} = \frac{\partial u}{\partial z} + \varepsilon^2 \frac{\partial w}{\partial x}. \quad (4d)$$

The boundary conditions at the ice surface, $z = s$, are

$$-(\varepsilon^2 \tau_{xx} - \varepsilon p)s_x + \tau_{xz} = 0, \quad (4e)$$

$$\varepsilon^2 (-\tau_{xz}h_x + \tau_{zz}) - \varepsilon p = 0, \quad (4f)$$

$$\frac{\partial s}{\partial t} + u \frac{\partial s}{\partial x} - w = \dot{b}, \quad (4g)$$

while at the bottom of the ice, $z = b$, we have

$$\text{either } u = w = 0, \quad \text{if } T < 0, \quad (4h)$$

$$\text{or } u_b = \gamma^{-1}\tau_b \quad \text{and} \quad w = u \frac{\partial b}{\partial x}, \quad \text{if } T = 0, \quad (4i)$$

with

$$u_b = u \left(1 + \varepsilon^2 \left(\frac{\partial b}{\partial x} \right)^2 \right)^{1/2}, \quad \tau_b = \frac{\left[1 - \varepsilon^2 \left(\frac{\partial b}{\partial x} \right)^2 \right] \tau_{xz} - 2\varepsilon^2 \frac{\partial b}{\partial x} \tau_{xx}}{1 + \varepsilon^2 \left(\frac{\partial b}{\partial x} \right)^2}. \quad (4j)$$

Energy conservation in the ice and in the bed reads, respectively

$$Pe \left(\frac{\partial T}{\partial t} + u \frac{\partial T}{\partial x} + w \frac{\partial T}{\partial z} \right) - \left(\varepsilon^2 \frac{\partial^2 T}{\partial x^2} + \frac{\partial^2 T}{\partial z^2} \right) = \alpha a \quad b < z < s, \quad (5a)$$

$$Pe \frac{\partial T}{\partial t} - \left(\varepsilon^2 \frac{\partial^2 T}{\partial x^2} + \frac{\partial^2 T}{\partial z^2} \right) = 0 \quad z < b, \quad (5b)$$

where the strain heating term a is defined as

$$a = 4\varepsilon^2 \left(\frac{\partial u}{\partial x} \right)^2 + 4\varepsilon^2 \left(\frac{\partial w}{\partial z} \right)^2 + \left(\frac{\partial u}{\partial z} \right)^2 + 2\varepsilon^2 \frac{\partial u}{\partial z} w_x + \varepsilon^4 \left(\frac{\partial w}{\partial x} \right)^2. \quad (5c)$$

Boundary conditions for the energy balance are

$$T = T_s \quad \text{on } z = s, \quad (5d)$$

$$-\frac{\partial T}{\partial z} \rightarrow \nu \quad \text{as } z \rightarrow -\infty, \quad (5e)$$

and

$$\text{either } [T] = \left[\frac{\partial T}{\partial z} \right]_+^+ = 0 \quad \text{on } z = b, \quad \text{if } T < 0, \quad (5f)$$

$$\text{or } T = 0 \quad \text{on } z = b, \quad \text{if } u_b > 0. \quad (5g)$$

In addition, we impose a reduced version of the enthalpy equation on the temperate side, which demands

$$m > 0 \quad \text{if } T = 0, \quad \text{on } z = b \quad (6a)$$

with basal melt rate

$$m = \left[\frac{\partial T}{\partial z} \right]_+^+ + \alpha \tau_b u_b. \quad (6b)$$

2 Supporting information for §3

2.1 Outer problem

A leading order approximation of the master model derived in §1.2 valid away from the transition point $x = x_{onset}$ can be obtained omitting terms of order $O(\varepsilon)$ and higher. This leads to the standard shallow ice approximation [3, 4]

$$u = \frac{1}{2} [h^2 - (s - z)^2] \left| \frac{\partial s}{\partial x} \right| + u_b, \quad \tau_b = h \left| \frac{\partial s}{\partial x} \right|, \quad (7a)$$

whereby we compute the mass flux as

$$q = \int_b^s u \, dz. \quad (7b)$$

The ice surface then evolves according to the diffusion equation

$$\frac{\partial s}{\partial t} + \frac{\partial q}{\partial x} = \dot{b}, \quad (7c)$$

while for the sliding velocity we have

$$\text{either } u = 0, \quad \text{if } T < 0, \quad (7d)$$

$$\text{or } u_b = \frac{1}{\gamma} \tau_b, \quad \text{if } T = 0. \quad (7e)$$

The vertical velocity is the solution to

$$\frac{\partial u}{\partial x} + \frac{\partial w}{\partial z} = 0 \quad \text{on } b < z < s, \quad (8a)$$

with boundary conditions at the bed, $z = b$,

$$\text{either} \quad w = 0, \quad \text{if } T < 0, \quad (8b)$$

$$\text{or} \quad u_b \frac{\partial b}{\partial x} - w = 0, \quad \text{if } T = 0. \quad (8c)$$

Lastly, omitting terms of order $O(\varepsilon^2)$, the leading order heat transport problem reads

$$Pe \left(\frac{\partial T}{\partial t} + u \frac{\partial T}{\partial x} + w \frac{\partial T}{\partial z} \right) - \frac{\partial^2 T}{\partial z^2} = \alpha a(x, z, t) \quad \text{for } b < z < s, \quad (9a)$$

$$Pe \frac{\partial T}{\partial t} - \frac{\partial^2 T}{\partial z^2} = 0 \quad \text{for } z < b, \quad (9b)$$

with strain heating $a = (\partial u / \partial z)^2$, and boundary conditions

$$T = T_s \quad \text{on } z = s, \quad (9c)$$

$$-\frac{\partial T}{\partial z} \rightarrow \nu \quad \text{as } z \rightarrow -\infty, \quad (9d)$$

and

$$\text{either} \quad [T]_-^+ = \left[\frac{\partial T}{\partial z} \right]_-^+ = 0 \quad \text{on } z = b \quad \text{if } T < 0, \quad (9e)$$

$$\text{or} \quad T = 0 \quad \text{on } z = b \quad \text{if } m > 0, \quad (9f)$$

where the basal melt rate reads

$$m = \left[\frac{\partial T}{\partial z} \right]_-^+ + \alpha \tau_b u_b. \quad (9g)$$

2.2 Boundary layer model

Consider the master model derived in §(1.2) and rescale dependent variables as

$$X = \varepsilon^{-1}(x - x_{onset}), \quad Z = z - b(x_{onset}), \quad (U, W) = (u, \varepsilon w), \quad H = h, \quad P = p, \quad \Theta = T. \quad (10)$$

We also assume that bed topography has structure only at the ice sheet scale, so in the boundary layer $b = b(x_{onset}) + O(\varepsilon)$. In addition we expand as

$$(U, W) = (U^{(0)}, W^{(0)}) + O(\varepsilon), \quad P = P^{(0)} + O(\varepsilon), \quad H = H^{(0)} + O(\varepsilon), \quad \Theta = \Theta^{(0)} + O(\varepsilon) \quad (11)$$

where surface elevation $H^{(0)}$ must be independent of X to leading order in order to conserve the mass flux across the boundary layer. This is analogous to the ice stream shear margin boundary layer in Haseloff et al. [5, 6], and simplifies the domain for the leading order problem to the strip $-\infty < X < \infty$, $-\infty < Z < H^{(0)}$, while structure in surface elevation at the ice thickness scale appears only at $O(\varepsilon)$.

Substituting the rescalings and expansions above into the non-dimensional version of the master model described in §(1.2), and omitting terms of $O(\varepsilon)$ and higher, we find the Stokes problem

$$\frac{\partial U^{(0)}}{\partial X} + \frac{\partial W^{(0)}}{\partial Z} = 0, \quad (12a)$$

$$\frac{\partial^2 U^{(0)}}{\partial X^2} + \frac{\partial^2 U^{(0)}}{\partial Z^2} - \frac{\partial P^{(0)}}{\partial X} = 0, \quad (12b)$$

$$\frac{\partial^2 W^{(0)}}{\partial X^2} + \frac{\partial^2 W^{(0)}}{\partial Z^2} - \frac{\partial P^{(0)}}{\partial Z} = 0, \quad (12c)$$

with boundary conditions

$$\frac{\partial U^{(0)}}{\partial Z} + \frac{\partial W^{(0)}}{\partial X} = W^{(0)} = 0 \quad \text{on } Z = H^{(0)}, \quad (12d)$$

$$W^{(0)} = 0 \quad \text{on } Z = 0, \quad (12e)$$

$$U_b^{(0)} = 0 \quad \text{on } Z = 0, \quad \text{if } \Theta^{(0)} < 0, \quad (12f)$$

$$U_b^{(0)} = \gamma^{-1} T_b^{(0)} \quad \text{on } Z = 0, \quad \text{if } \Theta^{(0)} = 0, \quad (12g)$$

where $U_b^{(0)} = U^{(0)}|_{Z=0}$, and $T_b^{(0)} = \partial U^{(0)} / \partial Z|_{Z=0}$. Matching conditions between the inner problem above and the shallow outer problem are

$$H^{(0)} = h(x_{onset}, t), \quad (U^{(0)}, W^{(0)}) \rightarrow (u(x_{onset}, z, t), 0) \quad \text{as } X \rightarrow \pm\infty, \quad (12h)$$

where u and h are the solution to the shallow ice model of §2.1.

Energy conservation up to an error of $O(\varepsilon)$ is

$$Pe_{BL} \left(U^{(0)} \frac{\partial \Theta^{(0)}}{\partial X} + W^{(0)} \frac{\partial \Theta^{(0)}}{\partial Z} \right) - \left(\frac{\partial^2 \Theta^{(0)}}{\partial X^2} + \frac{\partial^2 \Theta^{(0)}}{\partial Z^2} \right) = \alpha a \quad \text{for } 0 < Z < H^{(0)} \quad (13a)$$

$$\frac{\partial^2 \Theta^{(0)}}{\partial X^2} + \frac{\partial^2 \Theta^{(0)}}{\partial Z^2} = 0 \quad \text{for } -\infty < Z < 0, \quad (13b)$$

where the local Péclet number is $Pe_{BL} = \varepsilon^{-1} Pe \gg 1$, and strain heating reads

$$a = 2 \left(\frac{\partial U^{(0)}}{\partial X} \right)^2 + 2 \left(\frac{\partial W^{(0)}}{\partial Z} \right)^2 + \left(\frac{\partial U^{(0)}}{\partial Z} + \frac{\partial W^{(0)}}{\partial X} \right)^2. \quad (13c)$$

Boundary conditions are

$$\Theta^{(0)} = -1 \quad \text{on } Z = H^{(0)}, \quad (13d)$$

$$[\Theta^{(0)}]_-^+ = \left[\frac{\partial \Theta^{(0)}}{\partial Z} \right]_-^+ = 0 \quad \text{on } Z = 0, \quad \text{if } \Theta^{(0)} < 0, \quad (13e)$$

$$\Theta^{(0)} = 0 \quad \text{on } Z = 0, \quad \text{if } m^{(0)} > 0, \quad (13f)$$

$$-\frac{\partial \Theta^{(0)}}{\partial Z} = \nu \quad \text{as } Z \rightarrow -\infty, \quad (13g)$$

where the basal melt rate is

$$m^{(0)} = \left[\frac{\partial \Theta^{(0)}}{\partial Z} \right]_-^+ + \alpha T_b^{(0)} U_b^{(0)} \quad \text{on } Z = 0. \quad (13h)$$

In addition, the shallow ice outer thermal problem prescribes the temperature profile at the inflow boundary,

$$\lim_{X \rightarrow -\infty} \Theta^{(0)} = T(x_{onset}, z, t). \quad (13i)$$

2.3 The velocity field near the onset

We consider the mechanical problem given by eqs. (12a-12g) with the aim to derive an approximation for the velocity field valid at small distances from the frozen-molten transition located at $X = 0$. Introducing a stream function ψ such that

$$U^{(0)} = \frac{\partial \psi}{\partial Z}, \quad W^{(0)} = -\frac{\partial \psi}{\partial X}, \quad (14a)$$

it's straightforward to demonstrate that ψ satisfies the biharmonic equation,

$$\nabla^4 \psi = 0 \quad \text{on} \quad 0 < Z < 1, \quad -\infty < X < +\infty. \quad (14b)$$

As we are concerned with the behaviour of the velocity field near the bed and at small distances from the origin, we introduce a polar coordinate system (R, θ) , where $R = (X^2 + Z^2)^{1/2}$ is the distance from the origin, and $\theta \in [0, \pi]$ is the angle (taken positive anti-clockwise), with $\theta = 0$ denoting the bed on the temperate side of the transition, and seek to derive an expression for ψ when $R \rightarrow 0$ [see also 7, 8]. To this aim, we assume the separable ansatz

$$\psi = R^{\beta+2} \Psi(\theta), \quad (15a)$$

with β to be determined as part of the solution. Substituting into the biharmonic problem written in polar coordinates, and denoting with ' differentiation with respect to θ , the biharmonic equation reads

$$\Psi'''' - [\beta^2 + (\beta + 2)^2] \Psi'' + \beta^2 (\beta + 2)^2 \Psi = 0 \quad \text{on} \quad 0 < \theta < \pi, \quad (15b)$$

with boundary conditions along the bed

$$\Psi = 0 \quad \text{on} \quad \theta = 0, \pi, \quad (15c)$$

$$\Psi' = 0 \quad \text{on} \quad \theta = \pi, \quad (15d)$$

$$R^\beta [(\beta + 2)\Psi + \Psi''] = \gamma R^{\beta+1} \Psi' \quad \text{on} \quad \theta = 0, \quad (15e)$$

and general solution of the form

$$\Psi = A_1 \sin [(\beta + 2)(\pi - \theta)] + A_2 \cos [(\beta + 2)(\pi - \theta)] + B_1 \sin [\beta(\pi - \theta)] + B_2 \cos [\beta(\pi - \theta)], \quad (15f)$$

with A_1, A_2, B_1, B_2 integration constants.

We now seek to determine the constants using the boundary conditions (15c-15e). We start by noting that, in the limit of $R \rightarrow 0$, and with an error of $O(R)$, the sliding law eq. (15e) simplifies to free slip

$$\Psi'' = 0 \quad \text{on} \quad \theta = 0, \quad (15g)$$

meaning that the specific form of the sliding law is irrelevant to the leading order behaviour of the velocity field for $R \rightarrow 0$. Our problem is therefore equivalent to the leading order problem in Barcion and MacAyeal [7] who analyze a no slip-free slip transition; following their solution, we set $\beta = -1/2$ and obtain a stream function of the form

$$\Psi \sim c R^{3/2} \left[\sin \left(\frac{3\theta}{2} \right) + \sin \left(\frac{\theta}{2} \right) \right] \quad \text{for} \quad R \rightarrow 0, \quad (15h)$$

with the constant c to be determined from matching with the far field, $R \sim O(1)$. In terms of velocity (see definition 15h) the solution is

$$U^{(0)} \sim -\frac{c}{2} R^{1/2} \left[-5 \cos \left(\frac{\theta}{2} \right) + \cos \left(\frac{3\theta}{2} \right) \right], \quad W^{(0)} \sim -\frac{c}{2} R^{1/2} \csc \left(\frac{\theta}{2} \right) \sin^2(\theta) \quad \text{for} \quad R \rightarrow 0. \quad (15i)$$

A first observation regarding the velocity field (15i) is that the sliding velocity is continuous at the origin, $U^{(0)} \rightarrow 0$ as $R \rightarrow 0$, while the basal shear stress, $T_b^{(0)} = \partial U^{(0)} / \partial Z|_{Z=0} \sim R^{-1/2}$, is singular for $R \rightarrow 0$. We note however that the singularity is integrable, thus the local heat production remains bounded, as also noted by Barcilon and MacAyeal [7]. We therefore conclude that, from a mechanical perspective, a transition from frozen to molten bed is a viable boundary condition for the Stokes problem.

Note that Fowler [9] considered the same problem of flow near a transition from no slip to slip. He concluded that there should be a non-integrable singularity in strain heating, meaning such an abrupt transition would be physically impossible (see his eq. 41). Note however that the sliding law on $\theta = 0$ is replaced by a constant sliding velocity (his eq. 37₃) in his model. Unfortunately, a constant sliding velocity is inconsistent with the asymptotically reduced form of the sliding law, which we demonstrated collapses onto a free slip condition (so zero vertical shear stress) for small distances from the origin. Hence the velocity discontinuity and resulting point force claimed by Fowler [9] are spurious, and we conclude that the local flow problem is well-behaved.

2.4 The strong advection limit, $Pe_{BL} \gg 1$

2.4.1 Outer thermal problem

Let us consider the thermal problem at the ice thickness scale (13), and recall that the boundary layer Péclet number is large. Then, at large enough distance above the bed that the sliding velocity is $\sim O(1)$, a leading order approximation valid in both the cold- and temperate-based parts of the domain is

$$U \frac{\partial \Theta^{(0)}}{\partial X} + W \frac{\partial \Theta^{(0)}}{\partial Z} = O(Pe_{BL}^{-1}) \quad \text{for } 0 < Z < H^{(0)}, \quad (16a)$$

$$\Theta^{(0)} = 0 \quad \text{on } Z = 0, \quad (16b)$$

along with the matching condition (13i) at the inflow boundary, whereas in the bed we have

$$\Theta^{(0)} = -\nu Z \quad \text{for } Z < 0. \quad (16c)$$

The leading order dominant balance identified above holds so long as $(U^{(0)}, W^{(0)}) \sim O(1)$, which is clearly not the case in proximity of the bed, $Z \rightarrow 0$. This region must be dealt with by means of an advection-diffusion boundary layer nested within the ice thickness scale boundary layer; we will see that this new boundary layer stretches across the transition, all the way to the temperate region.

A diagram with the asymptotic structure of the thermal problem near the bed is provided in figure 1. In the following we derive leading order approximations for the near-bed boundary layers proceeding in the direction of the flow.

2.5 The advection-diffusion boundary layer on the cold side

We start our analysis considering the heat transport problem near the bed upstream of the transition, $X < 0$, in the region bounded from above by the yellow line in figure 1. We refer to this region as ‘cold advective-diffusive boundary layer’, and denote relevant variables in this region with ‘.

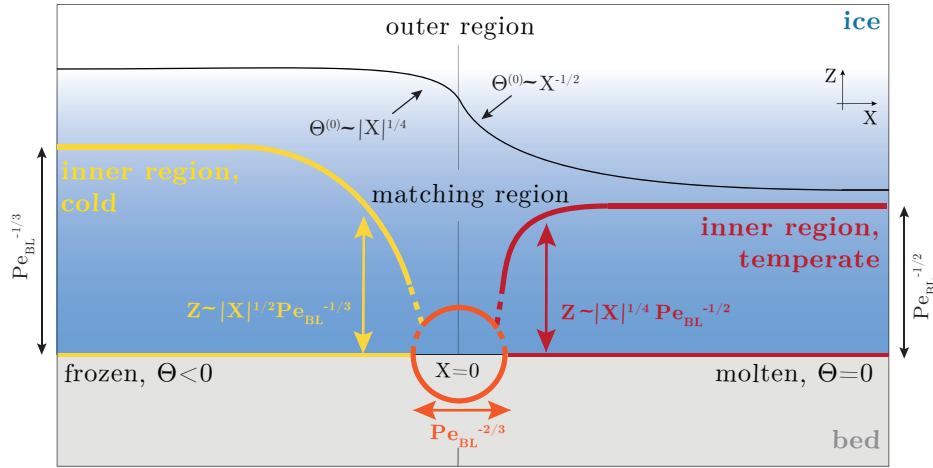


Figure 1: Illustration of the thermal boundary layers near the bed across a cold-temperate transition. Colored lines mark the advection-diffusion boundary layers, while the black curve represents an isotherm of the strongly advective outer problem (16).

2.5.1 Rescalings

We start by seeking scales for the velocity field in the boundary layer. Taylor-expanding the two components of velocity near the bed, along with basal no slip (12f), bed impermeability (12e), and mass conservation, eq. (12a), suggests to leading order

$$U^{(0)} \sim T_b^{(0)} Z, \quad W^{(0)} \sim -\frac{1}{2} \frac{\partial T_b^{(0)}}{\partial X} Z^2, \quad \text{with} \quad T_b^{(0)} \sim 2c|X|^{-1/2}, \quad \text{for} \quad Z \rightarrow 0, X < 0, \quad (17a)$$

while a vertical length scale is then obtained enforcing a balance between vertical diffusion and horizontal advection near the bed. Hence we put

$$X = r\acute{X}, \quad Z = Pe_{BL}^{-1/3} r^{1/2} \acute{Z}, \quad U^{(0)} = Pe_{BL}^{-1/3} \acute{U}, \quad W^{(0)} = Pe_{BL}^{-2/3} r^{-1/2} \acute{W}, \quad (17b)$$

where $r \leq O(1)$ marks distance from the origin.

In order to derive a temperature scale for the boundary layer, we require that the inner heat flux matches the heat flux imposed by the strongly advective outer temperature field in the matching region, that is $\acute{Z} \rightarrow \infty$ and $Z \rightarrow 0$. With the near-bed approximation of the velocity field (17a), isotherms of the outer problem (16) are the curves

$$Z \sim Z_0 |X|^{1/4} \quad \text{for} \quad Z > 0, X < 0. \quad (17c)$$

With $O(1)$ outer temperature, the outer heat flux behaves as

$$\frac{\partial \Theta^{(0)}}{\partial Z} \sim |X|^{-1/4} \quad \text{as} \quad Z \rightarrow 0, \quad (17d)$$

where we have assumed $Z_0 \sim O(1)$ to accommodate an $O(1)$ basal heat flux for the outer problem at $O(1)$ distances upstream of the origin, as required by eqs. (16). Then, matching inner and outer heat fluxes leads to the following rescaling for the boundary layer temperature

$$\Theta^{(0)} = Pe_{BL}^{-1/3} r^{1/4} \acute{\Theta} \quad \text{for} \quad Z > 0, \quad (17e)$$

while temperature remains unscaled in the bed,

$$\Theta^{(0)} = \acute{\Theta} \quad \text{for } Z < 0, \quad (17f)$$

which, substituted into continuity of temperature at the bed, eq.(13e₁), imply that basal temperature is at the melting point to leading order, while deviations from the melting point are small, and precisely $O(Pe_{BL}^{-1/3})$.

2.5.2 Leading order model

Informed by these rescalings, we expand dependent variables as

$$\begin{aligned} \acute{\Theta}(\acute{X}, \acute{Z}) &= \acute{\Theta}^{(0)} + o(1) && \text{for } \acute{Z} > 0, \\ \Theta(X, Z) &= \Theta^{(0)} + O\left(Pe_{BL}^{-1/3}\right) && \text{for } Z < 0, \\ (\acute{U}, \acute{W}) &= (\acute{U}^{(0)}, \acute{W}^{(0)}) + \left(O\left(Pe_{BL}^{-2/3}\right), O\left(Pe_{BL}^{-1}\right)\right). \end{aligned} \quad (18)$$

With leading order bed temperature at the melting point, the leading order problem in the bed decouples from the heat equation in the ice and can be solved analytically. The solution reads

$$\Theta^{(0)} = -\nu Z \quad \text{for } Z < 0, \quad (19)$$

which substituted into flux continuity at the bed (13e) yields a Neumann boundary condition for the leading order problem in the ice, i.e. $\partial \acute{\Theta}^{(0)} / \partial \acute{Z} = -\nu$ on $\acute{Z} = 0$.

The leading order problem in the ice up to an error of $O(Pe_{BL}^{-2/3})$ then reads

$$\acute{U}^{(0)} \frac{\partial \acute{\Theta}^{(0)}}{\partial \acute{X}} + \acute{W}^{(0)} \frac{\partial \acute{\Theta}^{(0)}}{\partial \acute{Z}} - \frac{\partial^2 \acute{\Theta}^{(0)}}{\partial \acute{Z}^2} = 0 \quad \text{for } 0 < \acute{Z} < +\infty, \quad \acute{X} < 0 \quad (20a)$$

with boundary and matching conditions

$$\left. \frac{\partial \acute{\Theta}^{(0)}}{\partial \acute{Z}} \rightarrow \frac{\partial \Theta^{(0)}}{\partial Z} \right|_{Z \rightarrow 0^+} \quad \text{as } \acute{Z} \rightarrow +\infty, \quad (20b)$$

$$-\frac{\partial \acute{\Theta}^{(0)}}{\partial \acute{Z}} = \nu \quad \text{on } \acute{Z} = 0, \quad (20c)$$

$$-\frac{\partial \acute{\Theta}^{(0)}}{\partial \acute{Z}} \rightarrow \nu \quad \text{as } \acute{X} \rightarrow -\infty. \quad (20d)$$

2.5.3 The temperature field remains bounded

The singularity of the basal shear stress for $|\acute{X}| \rightarrow 0$, and the consequent steepening of the outer heat flux ($\sim |X|^{-1/4}$ approaching the origin, $|\acute{X}| \rightarrow 0$), raise the issue as to whether the leading order model (20) admits a bounded solution, such that the far field temperature profile (20d) can be matched. The following analysis illustrates that this is actually the case.

Let us consider local forms of the velocity field, basal shear stress, and outer flux near the bed

$$\acute{U}^{(0)} = \acute{T}_b^{(0)} \acute{Z}, \quad \acute{W}^{(0)} = -\frac{\partial \acute{T}_b^{(0)}}{\partial \acute{X}} \frac{\acute{Z}^2}{2}, \quad \acute{T}_b^{(0)} = 2c|\acute{X}|^{-1/2}, \quad \frac{\partial \Theta^{(0)}}{\partial Z} = -\nu|X|^{-1/4}, \quad \text{on } \acute{Z}, Z = 0 \quad (21a)$$

and introduce the coordinate transformation to the characteristic coordinates (σ, η)

$$\eta = \left(\dot{T}_b^{(0)}\right)^{1/2} \dot{Z} = \frac{\dot{Z}}{|\dot{X}|^{1/4}}, \quad \sigma = -\frac{1}{2} \int_0^{\dot{X}} \dot{T}_b^{(0)}(\dot{X}')^{1/4} d\dot{X}' = \frac{2}{3} |\dot{X}|^{3/4}, \quad (21b)$$

where σ and η span the negative and positive half space, respectively. We further define a reduced temperature $\Theta^* = \dot{\Theta}^{(0)}(\sigma, \eta) + \nu\eta$, and substitute into eqs. (20). This yields

$$\eta \frac{\partial \Theta^*}{\partial \sigma} - \frac{\partial^2 \Theta^*}{\partial \eta^2} = 0 \quad \text{for } \eta > 0, \sigma < 0, \quad (22a)$$

with boundary and matching conditions

$$\frac{\partial \Theta^*}{\partial \eta} = F(\sigma) \quad \text{on } \eta = 0, \quad (22b)$$

$$\frac{\partial \Theta^*}{\partial \eta} \rightarrow 0 \quad \text{as } \eta \rightarrow +\infty, \quad (22c)$$

$$\frac{\partial \Theta^*}{\partial \eta} = 0 \quad \text{as } \sigma \rightarrow -\infty, \quad (22d)$$

where $F(\sigma) = \nu \left[1 - \left(\dot{T}_b^{(0)}\right)^{-1/2}\right]$.

It is now apparent that the solution to the problem (22) is well-behaved provided the function F also is. Recognizing that $F \sim O(1)$ as $\sigma \rightarrow 0$, and $F \rightarrow 0$ as $\sigma \rightarrow -\infty$, we conclude that the basal heat flux remains bounded throughout the domain, thus the far field temperature profile prescribed by (22d) can be matched. Therefore we expect that the solution exists and has no singularities.

In practice, the problem (22) can be solved in terms of Fourier transforms, provided the function F is extended to $\sigma > 0$. As σ is time-like, the form of F for $\sigma > 0$ is irrelevant to the solution in the negative half-space. It should be noted however that a closed form solution for Θ^* is likely not available due to spatially-varying basal boundary condition, eq. (22b).

2.6 The advection-diffusion boundary layer near the origin, $|X| \leq Pe_{BL}^{-2/3}$

The leading order model introduced in the previous section breaks down at distances from the origin $|X| \sim Pe_{BL}^{-2/3}$, where the assumption of shallowness of the boundary layer fails. This has to be dealt with via a rescaling of the horizontal coordinate, and effectively indicates the need for a distinct, non-shallow boundary layer. We anticipate that the dominant balance within the ice remains unchanged; the key difference with respect to the cold side lies instead in the fact that the non-shallow advection-diffusion boundary layer needs to be coupled to a diffusive boundary layer within the bed. This corresponds to the region bounded by the orange thick line in figure 1.

2.6.1 Rescalings

For the subsequent analysis we switch to a polar coordinate system centered on the origin, with radius $R = (X^2 + Z^2)^{1/2}$ and angle $\theta \in [0, 2\pi]$. In this region ($R \rightarrow 0$) the velocity is given by eq. (15i), so we put

$$(U_R^{(0)}, U_\theta^{(0)}) = r^{1/2}(\hat{U}_R, \hat{U}_\theta), \quad (23a)$$

where $r \ll 1$ is a typical non-dimensional distance, $(U_R^{(0)}, U_\theta^{(0)})$ are the radial and tangential components of the velocity field, and $\hat{\cdot}$ denotes boundary layer variables. Seeking a balance between advection and diffusion then yields the scale for the radius of the boundary layer,

$$r = Pe_{BL}^{-2/3}, \quad (23b)$$

while matching the heat flux with the shallow advection-diffusion layer on the cold side yields a scale for temperature, which we rescale as

$$\Theta^{(0)} = Pe_{BL}^{-1/2} \hat{\Theta}. \quad (23c)$$

We conclude by noting that the heat flux is asymptotically large, and scales as $\sim Pe_{BL}^{1/6}$ in this non-shallow boundary layer.

2.6.2 Leading order model

Informed by these scales, we expand dependent variables as

$$\begin{aligned} \hat{\Theta} &= \hat{\Theta}^{(0)} + O\left(Pe_{BL}^{-1/2}\right), \\ (\hat{U}_R, \hat{U}_\theta) &= (\hat{U}_R^{(0)}, \hat{U}_\theta^{(0)}) + O\left(Pe_{BL}^{-1/3}\right), \end{aligned} \quad (24a)$$

which yields the following leading order model, correct up to $O(Pe_{BL}^{-1/6})$:

$$\left(\hat{U}_R^{(0)}, \hat{U}_\theta^{(0)}\right) \cdot \left(\frac{\partial \hat{\Theta}^{(0)}}{\partial \hat{R}}, \frac{1}{\hat{R}} \frac{\partial \hat{\Theta}^{(0)}}{\partial \theta}\right) - \left(\frac{1}{\hat{R}} \frac{\partial \hat{\Theta}^{(0)}}{\partial \hat{R}} + \frac{\partial^2 \hat{\Theta}^{(0)}}{\partial \hat{R}^2} + \frac{1}{\hat{R}^2} \frac{\partial^2 \hat{\Theta}^{(0)}}{\partial \theta^2}\right) = 0 \quad \text{for } 0 < \theta < \pi, \quad (24b)$$

$$\frac{1}{\hat{R}} \frac{\partial \hat{\Theta}^{(0)}}{\partial \hat{R}} + \frac{\partial^2 \hat{\Theta}^{(0)}}{\partial \hat{R}^2} + \frac{1}{\hat{R}^2} \frac{\partial^2 \hat{\Theta}^{(0)}}{\partial \theta^2} = 0 \quad \text{for } \pi < \theta < 2\pi, \quad (24c)$$

with boundary conditions at the bed

$$\left[\hat{\Theta}^{(0)}\right]_-^+ = \left[\frac{\partial \hat{\Theta}^{(0)}}{\partial \theta}\right]_-^+ = 0, \quad \text{on } \theta = \pi, \quad (24d)$$

$$\hat{\Theta}^{(0)} = 0 \quad \text{on } \theta = 0, \quad (24e)$$

and matching conditions

$$-\frac{1}{\hat{R}} \frac{\partial \hat{\Theta}^{(0)}}{\partial \theta} \rightarrow \nu \quad \text{as } \hat{R} \rightarrow \infty, \text{ for } \theta = \pi, \quad (24f)$$

$$\frac{1}{\hat{R}} \frac{\partial \hat{\Theta}^{(0)}}{\partial \hat{R}} \rightarrow \frac{\partial \Theta^{(0)}}{\partial Z} \Big|_{Z \rightarrow 0} \quad \text{as } \hat{R} \rightarrow \infty, \text{ for } \theta \approx \pi/2, \quad (24g)$$

$$-\frac{1}{\hat{R}} \frac{\partial \hat{\Theta}^{(0)}}{\partial \theta} \rightarrow \nu \quad \text{as } \hat{R} \rightarrow \infty, \text{ for } \pi < \theta < 2\pi. \quad (24h)$$

Lastly, the inequality constraints reduce to

$$\frac{1}{\hat{R}} \left[\frac{\partial \hat{\Theta}^{(0)}}{\partial \theta}\right]_-^+ \geq 0 \quad \text{on } \theta = 0, \quad (24i)$$

$$\hat{\Theta}^{(0)} < 0 \quad \text{on } \theta = \pi. \quad (24j)$$

2.6.3 The inequality constraints can be satisfied locally

In order to show that the inequality constraints (24i-24j) can indeed be satisfied, we focus on deriving an asymptotic solution for temperature for $\hat{R} \rightarrow 0$. Since the leading order problem (24) becomes diffusion-dominated as we approach the origin, we follow the derivation by Schoof [8], which leads to a solution of the form

$$\hat{\Theta}^{(0)} = \sum_{m=0}^{\infty} a_m \hat{R}^{m+1/2} \sin((m+1/2)\theta) + b_m \hat{R}^{m+1} \sin((m+1)\theta) \quad \text{for } \hat{R} \rightarrow 0, \quad (25a)$$

where the coefficients a_m and b_m can be determined from asymptotic matching with the advection-diffusion problem (24).

We now seek to determine the coefficients a_m, b_m . In order to avoid singular freezing at the origin, and hence for the inequality constraints (24i-24j) to be satisfied locally, we demand $a_0 = 0$, $a_1 > 0$. This yields a leading order approximation

$$\hat{\Theta}^{(0)} \sim b_0 \hat{R} \sin(\theta) + a_1 \hat{R}^{3/2} \sin(3\theta/2) + O(\hat{R}^2). \quad (25b)$$

We are now going to demonstrate that the latter approximation satisfies the inequality constraints provided $a_1 > 0$. In fact, temperature along the bed on the cold side is

$$\hat{\Theta}^{(0)}(\theta = \pi) \sim -a_1 \hat{R}^{3/2} \quad \text{on } \theta = \pi, \quad (25c)$$

which is negative for $a_1 > 0$, thus satisfying the cold side inequality, eq. (24j). The net heat flux into the bed on the temperate side instead reads

$$\frac{\partial \hat{\Theta} / \partial \theta|_{\theta=0} - \partial \hat{\Theta} / \partial \theta|_{\theta=2\pi}}{\hat{R}} \sim 3a_1 \hat{R}^{1/2}, \quad (25d)$$

which is positive if $a_1 > 0$, thus satisfying the temperate side inequality eq. (24i). We thus conclude that it is possible to satisfy the inequality constraints (24i-24j) simultaneously in a region of radius $R < Pe_{BL}^{-2/3}$ near the origin at the cost of suppressing the leading order term in the expansion (25a).

Due to the time-like nature of the horizontal coordinate in the shallow advection-diffusion boundary layer that feeds the near-origin region (eqs. 20), the requirement that singular terms are suppressed in the solution for this region can be met only by tuning the inflow temperature profile (where the degree of freedom is really the deviation of basal temperature from the melting point) for $\hat{X} \rightarrow -\infty$. This leads to the complication that the local analysis above does not guarantee that the inequality constraints can be satisfied globally, on either sides of the transition. We will show later on (sec. 2.8) by means of numerical solution that this is actually the case, as in, the inequality constraints can be satisfied locally but are violated globally.

2.7 The advection-diffusion boundary layer on the temperate side

On the downstream side of the transition, $X > 0$, and at distances from the origin $X > Pe_{BL}^{-2/3}$, the circular advection-diffusion boundary layer described in §(2.6) is connected to a shallow advection-diffusion boundary layer that extends along the bed down to the downstream far field, $X \rightarrow +\infty$. This is the region bounded by red curves in figure 1, and we denote relevant variables in this region with \cdot .

2.7.1 Rescalings

We start by seeking scales for the velocity field. Taylor-expanding the two components of the velocity near the bed, and using the solution for the sliding velocity obtained from (15i) evaluated on $\theta = 0$ along with bed impermeability and mass conservation, eqs. (12e, 12a), suggests to leading order

$$U^{(0)} \sim U_b^{(0)} \sim 2X^{1/2} \quad W \sim -\frac{\partial U_b^{(0)}}{\partial X}Z \sim -X^{-1/2}Z, \quad \text{for } Z \rightarrow 0, X > 0, \quad (26a)$$

while a vertical length scale is obtained balancing horizontal advection and vertical diffusion in the boundary layer. Hence we put

$$X = r\dot{X}, \quad Z = Pe_{BL}^{-1/2}r^{1/4}\dot{Z}, \quad U^{(0)} = r^{1/2}\dot{U}, \quad W^{(0)} = Pe_{BL}^{-1/2}r^{-1/4}\dot{W}, \quad (26b)$$

where $r \leq O(1)$ denotes distance from the origin.

Next, we derive a scale for temperature in the boundary layer by demanding that the heat flux in the boundary layer matches the heat flux in the near field of the advection-only outer problem. Recalling that on the temperate side the outer problem satisfies the Q -equation

$$Q^{(0)}\frac{\partial U_b^{(0)}}{\partial X} - U_b^{(0)}\frac{\partial Q^{(0)}}{\partial X} = 0, \quad Q = -\frac{\partial \Theta^{(0)}}{\partial Z}\bigg|_{Z=0}, \quad (26c)$$

and therefore the outer heat flux behaves as

$$\frac{\partial \Theta^{(0)}}{\partial Z} \sim Pe_{BL}^{1/2}X^{1/2} \quad \text{as } Z \rightarrow 0 \quad (26d)$$

(where the constant $Pe_{BL}^{1/2}$ is chosen in such a way to allow matching between the non-shallow advection diffusion layer around the origin and the advection only far field for $X > 0$), matching inner and outer fluxes yields

$$\Theta^{(0)} = r^{3/4}\dot{\Theta}. \quad (26e)$$

We note that the rescalings derived above imply that the heat flux in the boundary layer is large at $O(1)$ distances from the origin, and precisely of order $O(Pe_{BL}^{1/2})$.

2.7.2 Leading order model

Informed by these scales, we expand dependent variables as

$$\begin{aligned} \dot{\Theta}(\dot{X}, \dot{Z}) &= \dot{\Theta}^{(0)} + o(1), \\ (\dot{U}, \dot{W}) &= (\dot{U}^{(0)}, \dot{W}^{(0)}) + O(Pe_{BL}^{-1/2}), \end{aligned} \quad (27)$$

which, substituted into the master model of §(1.2), yield the following leading order model correct up to order $O(Pe_{BL}^{-1})$

$$\dot{U}^{(0)}\frac{\partial \dot{\Theta}^{(0)}}{\partial \dot{X}} + \dot{W}^{(0)}\frac{\partial \dot{\Theta}^{(0)}}{\partial \dot{Z}} - \frac{\partial^2 \dot{\Theta}^{(0)}}{\partial \dot{Z}^2} = 0 \quad \text{for } 0 < \dot{Z} < +\infty, \quad (28a)$$

with boundary and matching conditions

$$\dot{\Theta}^{(0)} = 0 \quad \text{on } \dot{Z} = 0, \quad (28b)$$

$$\frac{\partial \dot{\Theta}^{(0)}}{\partial \dot{Z}} \rightarrow \frac{\partial \hat{\Theta}^{(0)}}{\partial \hat{Z}} \quad \text{as } \dot{X} \rightarrow 0, \quad \hat{X} \rightarrow +\infty, \quad (28c)$$

$$\frac{\partial \dot{\Theta}^{(0)}}{\partial \dot{Z}} \rightarrow \frac{\partial \Theta^{(0)}}{\partial Z}\bigg|_{Z \rightarrow 0} \quad \text{as } \dot{Z} \rightarrow \infty, \quad (28d)$$

while the leading order heat transport problem in the bed admits solution

$$\dot{\Theta}^{(0)} = -\nu Z \quad \text{for } Z < 0. \quad (28e)$$

Finally, the leading order basal energy budget, correct up to order $O(Pe_{BL}^{-1/2})$, requires

$$\left. \frac{\partial \dot{\Theta}^{(0)}}{\partial \dot{Z}} \right|_{\dot{Z}=0} \geq 0, \quad (28f)$$

which cannot possibly be satisfied for the heat flux is certainly into the ice. We therefore expect freezing to occur at $O(1)$ distances from the origin as a result of the steepening of the basal heat flux, consistently with the prediction from the much simpler analysis based on the Q -equation that we presented in the main text, §3b.

2.8 Numerical solution of the ice thickness scale problem

In this section we illustrate the behaviour of the leading order model derived in sections 2.5-2.7 by means of a numerical solution. Instead of considering the different leading order boundary layer models separately, we solve numerically the underlying ice thickness scale problem (12-13) with $Pe_{BL} \gg 1$ and $\alpha, \gamma, \nu \sim O(1)$. The numerical scheme presented below has been verified both against analytical solutions derived above and against numerical results produced with Elmer/Ice at comparable grid resolution.

2.8.1 Model reformulation

To facilitate the solution of the mechanical model, we reformulate the Stokes problem (12) in terms of a streamfunction ψ defined as

$$U^{(0)} = \frac{\partial \psi}{\partial Z}, \quad W^{(0)} = -\frac{\partial \psi}{\partial X}, \quad (29a)$$

and vorticity

$$\omega = \frac{\partial^2 \psi}{\partial X^2} + \frac{\partial^2 \psi}{\partial Z^2} \quad (29b)$$

In addition, and with the objective to reduce the number of parameters, we introduce the rescalings

$$(Z^*, X^*, H^{(0)*}) = (Z, X, H^{(0)})/H^{(0)}, \quad \psi^* = \psi/q^{(0)}, \quad \omega^* = \omega(H^{(0)})^2/q^{(0)}, \quad (29c)$$

$$(U^{*(0)}, W^{*(0)}) = (U^{(0)}, W^{(0)})H^{(0)}/q^{(0)}, \quad \Theta^{*(0)} = \Theta^{(0)}, \quad (29d)$$

$$(\nu^*, \gamma^*) = (\nu, \gamma)H^{(0)}, \quad \alpha^* = \alpha(q^{(0)}/H^{(0)})^2, \quad (29e)$$

where $H^{(0)}$ and $q^{(0)}$ are the leading order ice thickness and mass flux, which we recall to be constant in the boundary layer.

Then, with the rescalings above and following Batchelor [10], and also dropping asterisks for simplicity, the Stokes problem can be rewritten in terms of vorticity and streamfunction as

$$\nabla^2 \psi = \omega, \quad (30a)$$

$$\nabla^2 \omega = 0, \quad (30b)$$

on $0 < Z < 1, -\infty < X < \infty$, with boundary conditions at the surface and at the base

$$\psi = 1 \quad \text{on } Z = 1, \quad (30c)$$

$$\omega = 0 \quad \text{on } Z = 1, \quad (30d)$$

$$\psi = 0 \quad \text{on } Z = 0, \quad (30e)$$

$$\frac{\partial \psi}{\partial Z} = 0 \quad \text{on } Z = 0 \quad \text{if } \Theta^{(0)} < 0, \quad (30f)$$

$$\omega = \gamma \frac{\partial \psi}{\partial Z} \quad \text{on } Z = 0 \quad \text{if } \Theta^{(0)} = 0, \quad (30g)$$

while matching with the shallow ice far field is ensured by demanding

$$\frac{\partial \psi}{\partial X} = \frac{\partial \omega}{\partial X} = 0 \quad \text{as } X \rightarrow \pm \infty. \quad (30h)$$

As for the thermal problem (13), the rescaled problem is

$$Pe_{BL} \left(U^{(0)} \frac{\partial \Theta^{(0)}}{\partial X} + W^{(0)} \frac{\partial \Theta^{(0)}}{\partial Z} \right) - \left(\frac{\partial^2 \Theta^{(0)}}{\partial X^2} + \frac{\partial^2 \Theta^{(0)}}{\partial Z^2} \right) = \alpha a \quad \text{for } 0 < Z < 1 \quad (31a)$$

$$\frac{\partial^2 \Theta^{(0)}}{\partial X^2} + \frac{\partial^2 \Theta^{(0)}}{\partial Z^2} = 0 \quad \text{for } -\infty < Z < 0, \quad (31b)$$

where strain heating is the sum of an extensional contribution (a^E) and a shearing contribution (a^S)

$$a = a^E + a^S, \quad a^E = 4 \left(\frac{\partial^2 \psi}{\partial Z \partial X} \right)^2, \quad a^S = \left(\frac{\partial^2 \psi}{\partial Z^2} - \frac{\partial^2 \psi}{\partial X^2} \right)^2. \quad (31c)$$

Boundary conditions are

$$\Theta^{(0)} = T_s \quad \text{on } Z = 1, \quad (31d)$$

$$[\Theta^{(0)}]_-^+ = \left[\frac{\partial \Theta^{(0)}}{\partial Z} \right]_-^+ = 0 \quad \text{on } Z = 0, \quad \text{if } \Theta^{(0)} < 0, \quad (31e)$$

$$\Theta^{(0)} = 0 \quad \text{on } Z = 0, \quad \text{if } m^{(0)} > 0, \quad (31f)$$

$$-\frac{\partial \Theta^{(0)}}{\partial Z} = \nu \quad \text{as } Z \rightarrow -\infty, \quad (31g)$$

where the basal melt rate is

$$m^{(0)} = \left[\frac{\partial \Theta^{(0)}}{\partial Z} \right]_-^+ + \alpha T_b^{(0)} U_b^{(0)} \quad \text{on } Z = 0, \quad (31h)$$

with

$$T_b^{(0)} = \omega(Z = 0), \quad U_b^{(0)} = \frac{\partial \psi}{\partial Z} \Big|_{Z=0}. \quad (31i)$$

In addition, at the inflow boundary the temperature profile is prescribed by the advection-diffusion problem at the outer scale

$$\lim_{X \rightarrow -\infty} \Theta^{(0)} = T_{inflow}. \quad (31j)$$

In the absence of a closed form solution for the outer temperature field in the ice, and consistently with the asymptotic analysis of the inner thermal problem that suggests that small ($O(Pe_{BL}^{-1/3})$) deviations of bed temperature from the melting point are the only important aspect of the far field temperature profile, we put

$$T_{inflow} = \begin{cases} T_{b,\infty} - \nu Z, & \text{for } Z < 0, \\ (T_{b,\infty} - \nu Z)(1 - \theta) + \theta T_s, & \text{for } Z > 0, \end{cases} \quad (31k)$$

where $T_{b,\infty}$ is an adjustable parameter and $\theta(Z)$ is a smooth, monotonic function defined in $[0, 1]$ such that $\theta(0) = 0$ and $\theta(1) = 1$; in our computations we take

$$\theta = \exp(2\varepsilon_T) \exp\left[\frac{2\varepsilon_T}{(-2 + Z)Z}\right], \quad \varepsilon_T > 0. \quad (31l)$$

Lastly, and we have assumed without loss of generality that the transition is from frozen to molten bed, so

$$U_b^{(0)} = 0 \quad \text{on } X < 0, \quad \Theta^{(0)} = 0 \quad \text{on } X > 0, \quad Z = 0. \quad (31m)$$

2.8.2 Discretization

We discretize our model using finite volumes; for the mechanical problem the computational domain is the strip $-L_h^m < X < L_h^m$, and $0 < Z < 1$ (with $L_h > 1$), where we define a regular, two-dimensional, rectilinear grid locally refined near the ice-bed interface (in the vertical direction) and near the origin (in the horizontal direction). The grid has $2N_h$ grid points in the horizontal and N_v^i grid points in the vertical, with ψ and ω defined at cell centres. The ice-bed contact, $Z = 0$, and the ice surface $Z = 1$ are cell boundaries, and so are inflow and outflow boundaries, located at $X = \pm L_h$, as well as the transition itself, $X = 0$.

We label ψ -grid points by indices $\alpha = 1, 2, \dots, 2N_h$ and $\beta = 1, 2, \dots, N_v^i$, so that $\alpha = 1/2, 2N_h + 1/2$ are the inflow and outflow boundaries, respectively; $\alpha = N_h + 1/2$ is the frozen-molten transition, and $\beta = 1/2, N_v^i + 1/2$ are the ice-bed interface and the ice surface. The spacing between ψ -grid points is $\Delta X_j, \Delta Z_k$, with $1 \leq j \leq 2N_h, 1 \leq k \leq N_v^i$, where the indices j, k are restricted to integer values. Lastly the position of grid points given by

$$Z_\beta = \left[\left(\beta - \frac{1}{2} \right) \frac{1}{N_v^i} \right]^m, \quad (32a)$$

$$X_\alpha = \begin{cases} - \left| \left(\alpha - \frac{1}{2} \right) \frac{L_h}{N_h} - L_h \right|^m & \text{if } \alpha \leq N_h, \\ \left[\left(\alpha - \frac{1}{2} - N_h \right) \frac{L_h}{N_h} \right]^m & \text{if } \alpha > N_h, \end{cases} \quad (32b)$$

where $m \geq 1$, and $m = 1$ denotes an evenly spaced grid.

For the temperature field, our computational domain is the strip $-L_h^m < X < L_h^m$, and $-L_v^m < Z < 1$ (with $L_h, L_v > 1$), where we define a regular, two-dimensional, rectilinear grid locally refined near the ice-bed interface (in the vertical direction) and near the origin (in the horizontal direction). The grid has $2N_h + 1$ grid points in the horizontal and $N_v^i + N_v^b + 1$ grid points in the vertical, with Θ defined at cell centres (where we have dropped superscripts for simplicity). Note that the Θ -grid is staggered with respect to the ψ -grid, so that Θ -nodes are located on ψ cell boundaries.

Accordingly, the ice-bed contact, the ice surface, inflow and outflow boundaries, as well as the frozen molten transition are all cell centres for the Θ -grid.

We label Θ -grid points by indices $\alpha = 1/2, 3/2, \dots, 2N_h + 1/2$ and $\beta = -N_v^b + 1/2, -N_v^b + 3/2, \dots, N_v^i + 1/2$, so that $\alpha = 1/2, 2N_h + 1/2$ are the inflow and outflow boundaries, respectively, $\alpha = N_h + 1/2$ is the frozen-molten transition, and $\beta = 1/2, N_v^i + 1/2$ are the ice-bed interface and the ice surface. The spacing between Θ -grid points is ΔX_j , ΔZ_k , with $1 \leq j \leq 2N_h + 1$, $1 \leq k \leq N_v^i + N_v^b + 1$, where the indices j, k are restricted to integer and positive values. Lastly the position of grid points is given by

$$Z_{\beta/2} = \begin{cases} \left[\left(\beta - \frac{1}{2} \right) \frac{1}{N_v^i} \right]^m & \text{for } 1/2 \leq \beta \leq N_v^i + 1/2, \\ - \left| \left(\beta - \frac{1}{2} \right) \frac{L_v}{N_v^b} \right|^m & \text{for } -N_v^b + 1/2 \leq \beta < 1/2, \end{cases} \quad (32c)$$

$$X_{\alpha/2} = \begin{cases} - \left| \left(\alpha - \frac{1}{2} \right) \frac{L_h}{N_h} - L_h \right|^m & \text{for } 1/2 \leq \alpha \leq N_h + 1/2, \\ \left[\left(\alpha - \frac{1}{2} - N_h \right) \frac{L_h}{N_h} \right]^m & \text{for } N_h + 1/2 < \alpha < 2N_h + 1/2. \end{cases} \quad (32d)$$

Mechanical problem

For the biharmonic problem (30a-30b) we use a second-order centered scheme both in the horizontal and in the vertical, so in discrete form we get

$$\frac{1}{\Delta X_j} \left[\frac{2(\psi_{j+1,k} - \psi_{j,k})}{\Delta X_{j+1} + \Delta X_j} - \frac{2(\psi_{j,k} - \psi_{j-1,k})}{\Delta X_j + \Delta X_{j-1}} \right] + \frac{1}{\Delta Z_k} \left[\frac{2(\psi_{j,k+1} - \psi_{j,k})}{\Delta Z_{k+1} + \Delta Z_k} - \frac{2(\psi_{j,k} - \psi_{j,k-1})}{\Delta Z_k + \Delta Z_{k-1}} \right] = \omega_{j,k}, \quad (33a)$$

$$\frac{1}{\Delta X_j} \left[\frac{2(\omega_{j+1,k} - \omega_{j,k})}{\Delta X_{j+1} + \Delta X_j} - \frac{2(\omega_{j,k} - \omega_{j-1,k})}{\Delta X_j + \Delta X_{j-1}} \right] + \frac{1}{\Delta Z_k} \left[\frac{2(\omega_{j,k+1} - \omega_{j,k})}{\Delta Z_{k+1} + \Delta Z_k} - \frac{2(\omega_{j,k} - \omega_{j,k-1})}{\Delta Z_k + \Delta Z_{k-1}} \right] = 0. \quad (33b)$$

Regarding boundary condition, for $j = 1, 2N_h$ the equations above require both ω and ψ at the fictitious grid points $\alpha = j - 1/2 = 1/2$ and $\alpha = j + 1/2 = 2N_h + 1/2$. Here the far field conditions (30h) apply, so we put

$$\psi_{2N_h+1/2} = \psi_{2N_h-1/2}, \quad \psi_{1/2} = \psi_{3/2}, \quad \omega_{2N_h+1/2} = \omega_{2N_h-1/2}, \quad \omega_{1/2} = \omega_{3/2}. \quad (33c)$$

At the ice surface, $\beta = k + 1/2 = N_v^i + 1/2$, boundary conditions (30c) apply, so we put

$$\begin{aligned} \frac{2(\psi_{j,k+1} - \psi_{j,k})}{\Delta Z_{k+1} + \Delta Z_k} = & 2 \frac{(\Delta Z_{k-1}^2 + 4\Delta Z_k \Delta Z_{k-1} + 3\Delta Z_k^2)}{\Delta Z_k(\Delta Z_k + \Delta Z_{k-1})(2\Delta Z_k + \Delta Z_{k-1})} & \text{for } k = N_v^i, \\ & + 2 \frac{\Delta Z_k^2 \psi_{j,k-1} - (\Delta Z_{k-1} + 2\Delta Z_k)^2 \psi_{j,k}}{\Delta Z_k(\Delta Z_k + \Delta Z_{k-1})(2\Delta Z_k + \Delta Z_{k-1})} \end{aligned} \quad (33d)$$

$$\frac{2(\omega_{j,k+1} - \omega_{j,k})}{\Delta Z_{k+1} + \Delta Z_k} = 2 \frac{\Delta Z_k^2 \omega_{j,k-1} - (\Delta Z_{k-1} + 2\Delta Z_k)^2 \omega_{j,k}}{\Delta Z_k(\Delta Z_k + \Delta Z_{k-1})(2\Delta Z_k + \Delta Z_{k-1})} \quad \text{for } k = N_v^i, \quad (33e)$$

where we have used a second-order accurate polynomial extrapolation on the boundary to compute fluxes there. Similarly, to satisfy the boundary conditions (30e-30g) at the bed, $\beta = k - 1/2 = 1/2$,

we put

$$\frac{2(\psi_{j,k} - \psi_{j,k-1})}{\Delta Z_k + \Delta Z_{k-1}} = -2 \frac{\Delta Z_k^2 \psi_{j,k+1} - (\Delta Z_{k+1} + 2\Delta Z_k)^2 \psi_{j,k}}{\Delta Z_k(\Delta Z_k + \Delta Z_{k+1})(2\Delta Z_k + \Delta Z_{k+1})} \quad \text{for } k = 1, \quad (33f)$$

$$\begin{aligned} \frac{2(\omega_{j,k} - \omega_{j,k-1})}{\Delta Z_k + \Delta Z_{k-1}} = & -2 \frac{(\Delta Z_{k+1}^2 + 4\Delta Z_k \Delta Z_{k+1} + 3\Delta Z_k^2) \omega_{j,k-1/2}}{\Delta Z_k(\Delta Z_k + \Delta Z_{k+1})(2\Delta Z_k + \Delta Z_{k+1})} \\ & - 2 \frac{\Delta Z_k^2 \omega_{j,k+1} - (\Delta Z_{k+1} + 2\Delta Z_k)^2 \omega_{j,k}}{\Delta Z_k(\Delta Z_k + \Delta Z_{k+1})(2\Delta Z_k + \Delta Z_{k+1})} \end{aligned} \quad \text{for } k = 1, \quad (33g)$$

with

$$\omega_{j,1/2} = \begin{cases} \gamma \frac{2(\psi_{j,k} - \psi_{j,k-1})}{\Delta Z_k + \Delta Z_{k-1}} & \text{if } N_h + 1 \leq j \leq 2N_h, \\ \omega_{j,ghost} & \text{if } 1 \leq j \leq N_h, \end{cases} \quad (33h)$$

where $\omega_{j,ghost}$ is constrained by the no-slip condition at the bed (30f), which along with (33d) implies

$$\frac{2(\psi_{j,k} - \psi_{j,k-1})}{\Delta Z_k + \Delta Z_{k-1}} = -2 \frac{\Delta Z_k^2 \psi_{j,k+1} - (\Delta Z_{k+1} + 2\Delta Z_k)^2 \psi_{j,k}}{\Delta Z_k(\Delta Z_k + \Delta Z_{k+1})(2\Delta Z_k + \Delta Z_{k+1})} = 0 \quad \text{for } k = 1. \quad (33i)$$

Thermal problem

For $1 \leq j \leq 2N_h + 1$ and $N_v^b + 1 \leq k \leq N_v^i + N_v^b + 1$, energy conservation in the ice (31a) is discretized with a second-order centered schemes for the diffusive fluxes and the vertical advective flux, while we use a first-order upwind scheme for the horizontal advective flux, leading to

$$\begin{aligned} & \frac{U_{j,k-N_v^b-1/2} \Theta_{j-1/2,k-1/2} - U_{j-1,k-N_v^b-1/2} \Theta_{j-3/2,k-1/2}}{\Delta X_{j-1/2}} + \\ & \frac{1}{\Delta Z_{k-1/2}} \left[W_{j-1/2,k-N_v^b} \frac{\Theta_{j-1/2,k+1/2} \Delta Z_{k-1/2} + \Theta_{j-1/2,k-1/2} \Delta Z_{k+1/2}}{\Delta Z_{k+1/2} + \Delta Z_{k-1/2}} - \right. \\ & \quad \left. W_{j-1/2,k-N_v^b-1} \frac{\Theta_{j-1/2,k-1/2} \Delta Z_{k-3/2} + \Theta_{j-1/2,k-3/2} \Delta Z_{k-1/2}}{\Delta Z_{k-1/2} + \Delta Z_{k-3/2}} \right] - \\ & \frac{1}{Pe_{BL} \Delta Z_{k-1/2}} \left[\frac{2(\Theta_{j-1/2,k+1/2} - \Theta_{j-1/2,k-1/2})}{\Delta Z_{k+1/2} + \Delta Z_{k-1/2}} - \frac{2(\Theta_{j-1/2,k-1/2} - \Theta_{j-1/2,k-3/2})}{\Delta Z_{k-1/2} + \Delta Z_{k-3/2}} \right] - \\ & \frac{1}{Pe_{BL} \Delta X_{j-1/2}} \left[\frac{2(\Theta_{j+1/2,k-1/2} - \Theta_{j-1/2,k-1/2})}{\Delta X_{j+1/2} + \Delta X_{j-1/2}} - \frac{2(\Theta_{j-1/2,k-1/2} - \Theta_{j-3/2,k-1/2})}{\Delta X_{j-1/2} + \Delta X_{j-3/2}} \right] - \\ & \quad \frac{\alpha}{Pe_{BL}} a_{j-1/2,k-1/2} = 0, \end{aligned} \quad (34a)$$

while for $1 \leq k \leq N_v^b$, energy conservation in the bed (31b) is discretized with a second-order centered scheme leading to

$$\begin{aligned} & \frac{1}{\Delta Z_{k-1/2}} \left[\frac{2(\Theta_{j-1/2,k+1/2} - \Theta_{j-1/2,k-1/2})}{\Delta Z_{k+1/2} + \Delta Z_{k-1/2}} + \frac{2(\Theta_{j-1/2,k-1/2} - \Theta_{j-1/2,k-3/2})}{\Delta Z_{k-1/2} + \Delta Z_{k-3/2}} \right] - \\ & \frac{1}{\Delta X_{j-1/2}} \left[\frac{2(\Theta_{j+1/2,k-1/2} - \Theta_{j-1/2,k-1/2})}{\Delta X_{j+1/2} + \Delta X_{j-1/2}} - \frac{2(\Theta_{j-1/2,k-1/2} - \Theta_{j-3/2,k-1/2})}{\Delta X_{j-1/2} + \Delta X_{j-3/2}} \right] = 0. \end{aligned} \quad (34b)$$

Horizontal and vertical velocities are computed in terms of stream function as

$$U_{j,k-N_v^b-1/2} = 2 \frac{\psi_{j,k-N_v^b} - \psi_{j,k-N_v^b-1}}{\Delta Z_{k-N_v^b} + \Delta Z_{k-N_v^b-1}}, \quad (34c)$$

$$W_{j-1/2,k-N_v^b} = 2 \frac{\psi_{j,k-N_v^b} - \psi_{j-1,k-N_v^b}}{\Delta X_j + \Delta X_{j-1}}. \quad (34d)$$

For the heating term, it's worth noting that the extensional part, a^E , is naturally defined at Θ cell centres, as required, where the shearing part, a^S is defined at ψ cell centres; using a 4-point average for the shearing part, we put

$$a_{j-1/2,k-1/2} = a_{j-1/2,k-1/2}^E + \frac{a_{j,k-N_v^b-1}^S}{4\Delta Z_{k-N_v^b-1}\Delta X_j} + \frac{a_{j,k-N_v^b}^S}{4\Delta Z_{k-N_v^b}\Delta X_j} + \frac{a_{j-1,k-N_v^b-1}^S}{4\Delta Z_{k-N_v^b-1}\Delta X_{j-1}} + \frac{a_{j-1,k-N_v^b}^S}{4\Delta Z_{k-N_v^b}\Delta X_{j-1}}, \quad (34e)$$

where

$$a_{j-1/2,k-1/2}^E = \left[\frac{4}{\Delta X_j + \Delta X_{j-1}} \left(\frac{2(\psi_{j,k-N_v^b} - \psi_{j,k-N_v^b-1})}{\Delta Z_{k-N_v^b} + \Delta Z_{k-N_v^b-1}} - \frac{2(\psi_{j-1,k-N_v^b} - \psi_{j-1,k-N_v^b-1})}{\Delta Z_{k-N_v^b} + \Delta Z_{k-N_v^b-1}} \right) \right]^2, \quad (34f)$$

$$a_{j,k-N_v^b}^S = \left[\frac{1}{\Delta X_j} \left(\frac{2(\psi_{j+1,k-N_v^b} - \psi_{j,k-N_v^b})}{\Delta X_{j+1} + \Delta X_j} - \frac{2(\psi_{j,k-N_v^b} - \psi_{j-1,k-N_v^b})}{\Delta X_j + \Delta X_{j-1}} \right) + \frac{1}{\Delta Z_{k-N_v^b}} \left(\frac{2(\psi_{j,k-N_v^b+1} - \psi_{j,k-N_v^b})}{\Delta Z_{k-N_v^b+1} + \Delta Z_{k-N_v^b}} - \frac{2(\psi_{j,k-N_v^b} - \psi_{j,k-N_v^b-1})}{\Delta Z_{k-N_v^b} + \Delta Z_{k-N_v^b-1}} \right) \right]^2. \quad (34g)$$

Regarding boundary conditions, we start from the ice surface, $k = N_v^b + N_v^i + 1$. Recalling that Θ nodes lie on the ice surface itself, for these nodes we replace the conservation law with the Dirichlet condition (31d)

$$\Theta_{j-1/2,N_v^b+N_v^i+1/2} = T_S. \quad (34h)$$

Similarly, at the ice-bed interface on the temperate side, $k = N_v^b + 1$, $j > N_h$, we enforce the melting point temperature,

$$\Theta_{j-1/2,N_v^b+1/2} = 0 \quad \text{for } j > N_h. \quad (34i)$$

On the cold side, $j \leq N_h$, the discretization automatically ensures that the diffusive heat flux remains continuous across the bed, while bed impermeability implies that the vertical advective flux vanishes on the boundary, thus we put

$$W_{j-1/2,k-N_v^b-1} \frac{\Theta_{j-1/2,k-1/2}\Delta Z_{k-3/2} + \Theta_{j-1/2,k-3/2}\Delta Z_{k-1/2}}{\Delta Z_{k-1/2} + \Delta Z_{k-3/2}} = 0 \quad \text{for } k = N_v^b + 1. \quad (34j)$$

At the inflow boundary, $j = 1$, the solution must match the prescribed temperature profile (31k), so once more we replace the conservation law with the Dirichlet condition

$$\Theta_{1/2,k-1/2} = T_{inflow}(Z_{k-1/2}), \quad (34k)$$

while at the outflow boundary the boundary layer nature of the problem suggests

$$\Theta_{2N_h+3/2,k-1/2} = \Theta_{2N_h+1/2,k-1/2}, \quad a_{2N_h+1/2,k-1/2}^E = 0, \quad a_{2N_h+1,k}^S = a_{2N_h,k}^S. \quad (34l)$$

Solution

In the discrete problem above, we treat the inflow temperature profile as a one-parameter degree of freedom, where bed temperature $T_{b,\infty}$ is effectively arbitrary. Solving the boundary layer problem therefore amounts to finding $T_{b,\infty}$ such that the inequality constraints in (31e-31f) are satisfied at least locally near the transition point.

We do so by means of a bisection algorithm, similarly to Haseloff et al. [5, 6], whereby we seek to satisfy the discrete version of the inequality constraints (31e-31f) near the transition point, namely for the cold side, $j \leq N_h + 1$

$$\Theta_{N_v^b+1/2,j-1/2} < 0, \quad (35a)$$

and for the temperate side, $j > N_h + 1$,

$$2 \frac{\Theta_{N_v^b+3/2,j-1/2} - \Theta_{N_v^b+1/2,j-1/2}}{\Delta Z_{N_v^b+1/2} + \Delta Z_{N_v^b+3/2}} - 2 \frac{\Theta_{N_v^b+1/2,j-1/2} - \Theta_{N_v^b-1/2,j-1/2}}{\Delta Z_{N_v^b+1/2} + \Delta Z_{N_v^b-1/2}} + \alpha \omega_{1/2,j-1/2} U_{1/2,j-1/2} > 0. \quad (35b)$$

Note that in the latter expression we compute the heating term by averaging the sliding law (33h₁) and the basal velocity (given by 34c) over adjacent grid cells.

2.8.3 Results

Here we illustrate the behaviour of solutions to the discrete problem described in §(2.8.2); as we are interested in the behaviour of the leading order thermal problem derived in sections (2.5-2.7), we also set to zero the strength of strain heating, α , because the asymptotics show that strain heating is a higher order correction throughout the domain. The reader is referred to the main text, §3c, for solutions with finite α .

Figure 2 shows the solution with $\alpha = 0$: the velocity and temperature fields are displayed in panels (a) and (b) respectively, and the inequality constraints along the bed in panel (c). It's immediately obvious that, even though the inequality constraints are locally satisfied near the origin (inset of panel (c)), they are violated away from the origin both on the cold ($X < 0$, green curve) and temperate ($X > 0$ yellow curve) side of the transition, so the boundary layer problem appears to have no solution.

Let us examine our results in more detail: on the cold side ($X < 0$), bed temperature is consistently above the melting point except for a small region about the origin, $|X| < 0.001$; moreover, basal temperature decreases as the origin is approached, which along with the behaviour of isotherms above the bed (panel (b)) confirms that the advection-diffusion boundary layer cools down as the origin is approached. On the temperate side ($X > 0$), the basal energy budget remains positive for $X < 0.04$, and turns negative further away as predicted by the asymptotic analysis in sections (2.5-2.7).

Next, we focus on the solution of the thermal problem near the origin. We have shown in §2.6 that the analytical solution of the diffusion-only problem near the origin in general has leading order term $\sim R^{1/2}$, which however leads to singular freezing on the temperate side. We therefore concluded that suitable farfield conditions (that is, basal temperature at the inflow, $T_{b,\infty}$) must be such that the leading order term is suppressed, and therefore the inequality constraints can be satisfied at $O(R^{3/2})$. We now want to confirm this behaviour numerically.

Panel (d) of figure 2 illustrates the behaviour of basal temperature against distance from the origin for different values of $T_{b,\infty}$. Circles denote results from the numerics while solid lines are analytical approximations constructed with the first three terms of the analytical solution for the diffusion-only problem near the origin, eq. (25a). The actual solution (same as panels a-c) is for

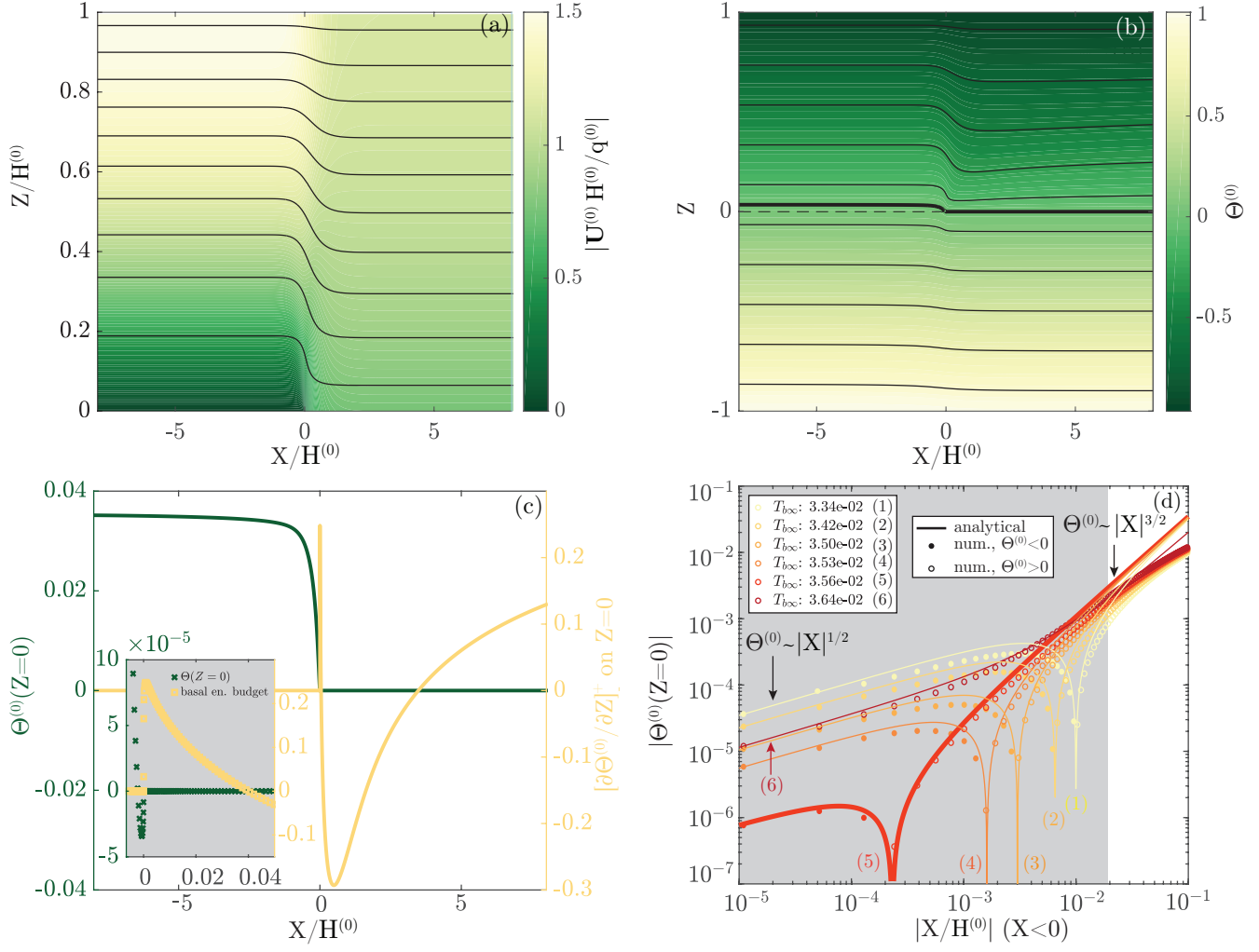


Figure 2: Numerical solution of the problem (12-13) with $Pe_{BL} = 200$, $\alpha = 0$, $\nu = 1$, $\gamma = 1$, $T_S = -1$, $T_{b\infty} = 0.0356$. Panel a: velocity field (color) and streamlines (black lines). Panel b: temperature field. Thin solid lines are isotherms (evenly spaced by $\Delta\Theta = 0.2$), the thick solid lines denotes the $\Theta = 0$ isotherm, and the dashed black line denotes the bed, $Z = 0$. Panel c (and inset): basal temperature and basal energy budget; the inset displays a zoom near the origin. Panel (d): basal temperature on the cold side as a function of distance from the origin for different values of $T_{b\infty}$.

$T_{b,\infty} = 0.0356$, and is marked with (5). The shaded area denotes the region with $R < Pe_{BL}^{-2/3}$, which is an upper bound for the region of validity of the analytical approximation.

A general note is that numerical (circles) and analytical (solid lines) solutions compare favorably, with the discrepancy increasing with distance from the origin as expected (the error of the approximation is of order $\sim O(R^{5/2})$). Changes in $T_{b,\infty}$ have two effects: first of all, as $T_{b,\infty}$ increases we observe a transition from negative basal temperature (closed circles) immediately upstream of the origin (curves 1-5) to positive basal temperature (open circles, curve 6). This also corresponds to a transition from singular freezing to a positive basal energy budget on the temperate side (not shown), thus suggesting that the value of $T_{b,\infty}$ that satisfies both inequalities is unique [see also 8]. Secondly, we observe that the portion of the solution that is approximated by the curve $\Theta^{(0)} \sim |X|^{1/2}$ can be reduced to a region near the origin that is comparable with the local grid spacing (curve 5), while it is larger for smaller (curves 1-4) or larger (curve 6) values of $T_{b,\infty}$. We are therefore confident that it is possible to find a value of $T_{b,\infty}$ such that the right analytical behaviour is recovered except within a region that is comparable with the numerical grid spacing.

3 Supporting information for §4

3.1 Freezing in the subtemperate region with $\delta \sim O(1)$

In this section we seek to derive a reduced heat transport model for the basal heat flux that holds in the case of subtemperate sliding with $\delta \sim O(1)$. Let us assume that the subtemperate region is short, meaning that basal temperature changes of $O(1)$ over distances comparable with the ice thickness. Over these short horizontal distances, and with ice sheet scale Péclet number $Pe \sim O(1)$, the heat transport problem is advection-dominated, and the leading order model (16a) applies within the ice. The key difference with respect to fully temperate sliding, or subtemperate sliding in the limit of $\delta \rightarrow 0$ is that here temperature changes along the bed, so the derivation of the standard Q -equation (§3b of the main text) no longer holds. We therefore seek to derive a generalized version of the Q -equation that accounts for spatially variable basal temperature.

We start from equation (16a), differentiate with respect to Z , and take the limit of $Z \rightarrow 0$; this yields

$$\frac{\partial U^{(0)}}{\partial Z} \frac{\partial \Theta^{(0)}}{\partial X} + U^{(0)} \frac{\partial}{\partial X} \left(\frac{\partial \Theta^{(0)}}{\partial Z} \right) + \frac{\partial W^{(0)}}{\partial Z} \frac{\partial \Theta^{(0)}}{\partial Z} + W \frac{\partial \Theta^{(0)}}{\partial Z} = 0 \quad \text{on } Z = 0. \quad (36a)$$

We now seek to simplify the latter expression. With impermeability of the bed (12e), and assuming sliding to be $\sim O(1)$, a Taylor expansion near the bed yields

$$U^{(0)} \sim U_b^{(0)} + O(Z), \quad W^{(0)} \sim \left. \frac{\partial W}{\partial Z} \right|_{Z=0} Z + O(Z^2) = -\frac{\partial U_b^{(0)}}{\partial X} Z + O(Z^2) \quad \text{for } Z \rightarrow 0, \quad (36b)$$

where we have used mass conservation (12a) to obtain the expression for $W^{(0)}$. Defining the basal heat flux as $Q = -\partial \Theta^{(0)} / \partial Z$, we obtain the generalized version of the steady state Q -equation

$$U_b^{(0)} \frac{\partial Q}{\partial X} = \frac{\partial U^{(0)}}{\partial Z} \frac{\partial \Theta^{(0)}}{\partial X} + \frac{\partial U_b^{(0)}}{\partial X} Q. \quad (36c)$$

Recalling that U_b is a monotonically increasing function of $\Theta^{(0)}$, that the heat flux is into the ice so $Q > 0$, and that the bed has to warm along the subtemperate region, it is straightforward to see that the rhs of eq. (36c) is positive. As a result, $\partial Q / \partial X > 0$ and larger than it would be if the bed was an isotherm, i.e., $\partial \Theta^{(0)} / \partial X = 0$.

Given that for the case with $\partial\Theta^{(0)}/\partial X = 0$ (that is, for $\delta = 0$) we argued that the basal heat flux has to become asymptotically large over finite distances downstream of sliding onset, thus leading to refreezing, we understand that the behaviour for $\delta \rightarrow 0$ is effectively a lower bound, hence refreezing must necessarily happen also for $\delta \sim O(1)$.

4 Supporting information for §5

4.1 Model reformulation in a stretched coordinate system

Let us consider the ice sheet scale model presented in §(2.1) modified with basal boundary conditions

$$[\partial T / \partial z]_-^+ = u_b = 0 \quad \text{if } T \leq 0, \quad (37a)$$

$$\left[\frac{\partial T}{\partial z} \right]_-^+ + \alpha u_b \tau_b = T = 0 \quad \text{if } u_b < \gamma^{-1} \tau_b, \quad (37b)$$

$$T = u_b - \gamma^{-1} \tau_b = 0 \quad \text{if } \left[\frac{\partial T}{\partial z} \right]_-^+ + \alpha u_b \tau_b > 0, \quad (37c)$$

and continuity requirements at subdomain boundaries

$$[q]_-^+ = [h]_-^+ = \left[\frac{\partial T}{\partial z} \right]_-^+ = 0, \quad (37d)$$

and denote the downstream and upstream boundaries of each subdomain with $x_d(t)$ and $x_u(t)$. Then we introduce the stretched coordinate system

$$\xi = \xi_0^i + \frac{x - x_u^i}{x_d^i - x_u^i}, \quad \eta = \frac{z - b}{h}, \quad \tau = t, \quad (38a)$$

which maps the length and height of each subdomain to the rectangular domain $\xi_0^i < \xi < \xi_0^i + 1$, $0 < \eta < 1$. We will take $\xi_0^i = i - 1$ for $i = (1, 2, 3)$ so that the ice divide is located at $\xi = 0$, the cold-subtemperate boundary at $\xi = 1$, the subtemperate-temperate boundary at $\xi = 2$, and the grounding line at $\xi = 3$ (see figure 3).

In the new coordinate system we have dependent variables

$$h^*(\xi, \tau) = h(x, t), \quad u^*(\xi, \eta, \tau) = u(x, z, t), \quad w^*(\xi, \eta, \tau) = w(x, z, t), \quad T^*(\xi, \eta, \tau) = T(x, z, t), \\ x_s^*(\xi, \tau) = x_s(t), \quad x_t^*(\xi, \tau) = x_s(t), \quad x_g^*(\xi, \tau) = x_g(t),$$

while bed elevation b remains a known function of $x(\xi, \tau)$. Then, under the chain rule, derivatives map to

$$\frac{\partial}{\partial x} = \frac{1}{x_d^{*,i} - x_u^{*,i}} \frac{\partial}{\partial \xi} - \frac{1}{h^*} \left(\frac{db}{dx} + \frac{\eta}{x_d^{*,i} - x_u^{*,i}} \frac{\partial h^*}{\partial \xi} \right) \frac{\partial}{\partial \eta}, \quad (38b)$$

$$\frac{\partial}{\partial z} = \frac{1}{h^*} \frac{\partial}{\partial \eta}, \quad (38c)$$

$$\frac{\partial}{\partial t} = \frac{\partial}{\partial \tau} + \frac{1}{x_d^{*,i} - x_u^{*,i}} \left[(\xi - (\xi_0^i + 1)) \frac{\partial x_u^{*,i}}{\partial \tau} - (\xi - \xi_0^i) \frac{\partial x_d^{*,i}}{\partial \tau} \right] \frac{\partial}{\partial \xi} \\ - \frac{\eta}{h^*} \left[\frac{\partial h^*}{\partial \tau} + \frac{1}{x_d^{*,i} - x_u^{*,i}} \left((\xi - 1) \frac{\partial x_u^{*,i}}{\partial \tau} - \xi \frac{\partial x_d^{*,i}}{\partial \tau} \right) \frac{\partial h^*}{\partial \xi} \right] \frac{\partial}{\partial \eta}. \quad (38d)$$

4.1.1 Ice thickness evolution

Dropping asterisks for simplicity, and applying the coordinate transformation above as well as the product rule, global mass conservation (7c) becomes

$$\frac{\partial}{\partial \tau} [(x_d^i - x_u^i)h] + \frac{\partial q_e}{\partial \xi} - (x_d^i - x_u^i) \dot{b} = 0, \quad (39a)$$

with effective mass flux and effective velocity defined as

$$q_e = \int_0^1 u_e(\xi, \eta, \tau) d\eta, \quad u_e = u_d + u_b + u_a, \quad (39b)$$

where u_d is the shearing portion of the velocity profile,

$$u_d = -\frac{h^2}{2} [1 - (1 - \eta)^2] \left(\frac{db}{dx} + \frac{1}{x_d^i - x_u^i} \frac{\partial h}{\partial \xi} \right), \quad (39c)$$

u_a is an apparent velocity (independent of η) related to the motion of subdomain boundaries

$$u_a = [\xi - (\xi_0^i + 1)] \frac{\partial x_u^i}{\partial \tau} - (\xi - \xi_0^i) \frac{\partial x_d^i}{\partial \tau}, \quad (39d)$$

and u_b is the sliding velocity

$$u_b = 0 \quad \text{for } i = 1, \quad (39e)$$

$$u_b = \frac{1}{\alpha \tau_b} (Q - \nu) \quad \text{for } i = 2, \quad (39f)$$

$$u_b = \frac{1}{\gamma} \tau_b \quad \text{for } i = 3, \quad (39g)$$

with vertical shear stress

$$\tau_{xz} = -h(1 - \eta) \left(\frac{\partial b}{\partial x} + \frac{1}{x_d^i - x_u^i} \frac{\partial h}{\partial \xi} \right), \quad \tau_b = \tau_{xz}|_{\eta=0}. \quad (39h)$$

and basal heat flux

$$Q = - \frac{1}{h} \frac{\partial T}{\partial \eta} \Big|_{\eta=0}. \quad (39i)$$

Eq. (39a) with the constitutive relations above is the standard diffusion problem for h arising from shallow ice approximations. Rewriting the flux as $q_e = q + q_a$, where $q = q_d + q_b$ is the sum of the mass flux by shearing and by basal sliding while q_a is the apparent mass flux (that is $q_i = \int_0^1 u_i d\eta$, with $i = d, b, a$), and noting that q_a is continuous by construction at subdomain boundaries while it vanishes on $\xi = 0$, suitable boundary conditions are

$$q = 0 \quad \text{on } \xi = 0, \quad (39j)$$

$$[q]_-^+ = [h]_-^+ = 0 \quad \text{on } \xi = 1, \xi = 2, \quad (39k)$$

$$h = -\frac{\rho}{\rho_w} b \quad \text{on } \xi = 3, \quad (39l)$$

$$q = Q_g(h) \quad \text{on } \xi = 3. \quad (39m)$$

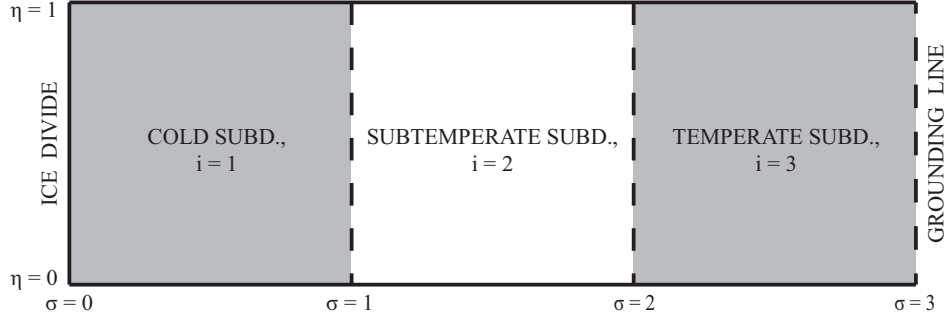


Figure 3: Schematic of the computational domain in the stretched coordinate system.

where the function Q_g is given by Schoof [11], and reads (translated to the current non - dimensionalization)

$$Q_g = q_0 \gamma^{-1/3} h^{5/2}, \quad q_0 = \varepsilon^{-1} \left(\frac{1 - \rho_w^{-1} \rho}{8} \right)^{1/2} \sim O(1). \quad (39n)$$

Note that, since the ice thickness at the grounding line is a known function of bed elevation through the flotation condition (39l), eq. (39m) effectively fixes the location of the grounding line, $x_g = x_d^3$.

4.1.2 Temperature evolution

Applying the same coordinate transformation to energy conservation within the ice, eq. (9a), as well as the product rule, yields

$$\frac{\partial}{\partial \tau} [(x_d^i - x_u^i) h T] + \frac{\partial}{\partial \xi} [u_e h T] + \frac{\partial}{\partial \eta} \left[(x_d^i - x_u^i) w_e T - \frac{(x_d^i - x_u^i)}{Pe h} \frac{\partial T}{\partial \eta} \right] = \frac{\alpha}{Pe} (x_d^i - x_u^i) \tau_{xz} \frac{\partial u}{\partial \eta}, \quad (40a)$$

with w_e the vertical effective velocity, defined as

$$w_e = w - u \left(\frac{db}{dx} + \frac{\eta}{x_d^i - x_u^i} \frac{\partial h}{\partial \xi} \right) - \eta \left[\frac{\partial h}{\partial \tau} + \frac{1}{x_d^i - x_u^i} \left[(\xi - (\xi_0^i + 1)) \frac{\partial x_u^i}{\partial \tau} - (\xi - \xi_0^i) \frac{\partial x_d^i}{\partial \tau} \right] \frac{\partial h}{\partial \xi} \right]. \quad (40b)$$

For the heat equation in the bed, we restrict ourselves to the simple case of a linear temperature profile with heat flux equal to the geothermal heat flux. This is effectively the solution to eq. (9b) in a steady state or in the limit of $Pe \ll 1$; as most of the following analyses are concerned with steady state computations, and also considering that both in the subtemperate and temperate region boundary values are independent of time, we disregard transient effects in the bed at the ice sheet scale. As a result, boundary conditions for the heat equation simplify to

$$T = T_S \quad \text{on } \eta = 1, \quad (40c)$$

$$-\frac{1}{h} \frac{\partial T}{\partial \eta} = \nu \quad \text{on } \eta = 0 \quad \text{for } i = 1, \quad (40d)$$

$$T = 0 \quad \text{on } \eta = 0 \quad \text{for } i = 2, 3, \quad (40e)$$

whereas on vertical domain boundaries we demand

$$\frac{\partial T}{\partial \xi} = 0 \quad \text{on } \xi = 0, \quad (40f)$$

$$[T]_-^+ = 0 \quad \text{on } \xi = 1, \xi = 2, \quad (40g)$$

which ensure no flux across the divide, and a continuous heat flux across subdomain boundaries.

To close the model, we need an evolution equation for w_e . We start by applying the coordinate transformation and the product rule to the local mass conservation, eq. (8a), which yields

$$\frac{\partial}{\partial \eta} \left[w - u \left(\frac{db}{dx} + \frac{\eta}{x_d^i - x_u^i} \frac{\partial h}{\partial \xi} \right) \right] + \frac{1}{x_d^i - x_u^i} \frac{\partial(uh)}{\partial \xi} = 0, \quad (41a)$$

with boundary condition at the bed, $\eta = 0$

$$w = 0 \quad \text{for } i = 1, \quad (41b)$$

$$w = u b_x, \quad \text{for } i = 2, 3. \quad (41c)$$

Then, substituting the definition (40b) into (41a), and also using the global mass conservation (39a) yields the desired evolution equation for w_e ,

$$\frac{\partial w_e}{\partial \eta} + \frac{1}{x_d^i - x_u^i} \frac{\partial}{\partial \xi} [u_d h - q_d] = -\dot{b}, \quad (42a)$$

with boundary condition at the bed

$$w_e = 0 \quad \text{on } \eta = 0. \quad (42b)$$

We note that, from a numerical perspective, eq. (42a) is preferable to (41a) because, provided the mass flux q is discretized consistently in eq. (39a) and in eq. (42a), then eq. (42a) automatically ensures that the vertical velocity field is mass-conserving.

4.1.3 Sub-domain boundaries

Lastly, we need constraints for the location of the cold-subtemperate and subtemperate-temperate boundaries. At these boundaries, the inequality constraints in eqs. (37a-37c) must hold simultaneously, that is

$$T = 0 \quad \text{on } \eta = 0, \xi = 1, \quad (43a)$$

$$\frac{1}{\alpha \tau_b} (Q - \nu) = \frac{1}{\gamma} \tau_b \quad \text{on } \xi = 2. \quad (43b)$$

These equalities effectively fix the location of cold-subtemperate ($x_s = x_d^1, x_u^2$) and subtemperate-temperate ($x_t = x_d^2, x_u^3$) boundaries. As we are not solving for enthalpy of the bed, we cannot enforce directly a positive basal energy budget on the temperate side. Rather, we will verify a posteriori that solutions satisfy this constraint.

4.2 Discretization

We discretize our model using finite volumes. We define a uniformly spaced, one-dimensional grid for h in each subdomain, with N_h^1 grid points in $0 < \xi < 1$, N_h^2 in $1 < \xi < 2$, and N_h^3 in $2 < \xi < 3$. The junctions $\xi = 1, 2$ as well as the grounding line and ice divide, $\xi = 0, 3$, are cell boundaries. We label h-grid points by indices $\alpha = 1, 2, \dots, N_h^1 + N_h^2 + N_h^3$ so $\alpha = 1/2$ is the ice divide, $\alpha = N_h^1 + 1/2$ is the cold-subtemperate boundary, $\alpha = N_h^1 + N_h^2 + 1/2$ is the subtemperate-temperate boundary, and $\alpha = N_h^1 + N_h^2 + N_h^3 + 1/2$ is the grounding line. The spacing between h -grid points is $\Delta \xi_j$

with $\Delta\xi_j = \Delta\xi^1$ for $1 \leq \alpha \leq N_h^1$, and similarly $\Delta\xi_j = \Delta\xi^2$ and $\Delta\xi_j = \Delta\xi^3$ for $N_h^1 \leq \alpha \leq N_h^1$ and $N_h^2 \leq \alpha \leq N_h^3$. The positions of grid points are

$$\xi_\alpha = \begin{cases} \left(\alpha - \frac{1}{2}\right) \Delta\xi^1 & \text{for } 1 \leq \alpha \leq N_h^1 \\ \left(N_h^1 - \frac{1}{2}\right) \Delta\xi^1 + \left(\alpha - N_h^1 - \frac{1}{2}\right) \Delta\xi^2 & \text{for } N_h^1 \leq \alpha \leq N_h^2 \\ \left(N_h^1 - \frac{1}{2}\right) \Delta\xi^1 + \left(N_h^2 - N_h^1 - \frac{1}{2}\right) \Delta\xi^2 + \left(\alpha - N_h^2 - \frac{1}{2}\right) \Delta\xi^3 & \text{for } N_h^2 \leq \alpha \leq N_h^3. \end{cases} \quad (44a)$$

For T and w_e we define a uniformly spaced, two-dimensional, vertically staggered grid, with N_h^1 grid points along the horizontal direction in $0 < \xi < 1$, N_h^2 in $1 < \xi < 2$, and N_h^3 in $2 < \xi < 3$, and N_v grid points along the vertical. The bed $\eta = 0$ and the ice surface $\eta = 1$ are w_e points, while the junctions $\xi = 1, 2$ as well as the grounding line and ice divide, $\xi = 0, 3$ are both T and w_e cell boundaries. Thus the T -grid and the w_e -grid are co-located with the h -grid.

We label T -grid points by indices $\alpha = 1, 2, \dots, N_h^1 + N_h^2 + N_h^3$ and $\beta = 1, 2, \dots, N_v$, while w_e -grid points with $\alpha = 1, 2, \dots, N_h^1 + N_h^2 + N_h^3$ and $\beta = 1/2, 3/2, \dots, N_v + 1/2$. So $\beta = 1/2$ is the bed and $\beta = N_v + 1/2$ is the ice surface. The horizontal spacing is identical to the spacing of the h -grid: the spacing between grid points with $1 \leq \alpha \leq N_h^1$ is $\Delta\xi^1$, and similarly $\Delta\xi^2$ and $\Delta\xi^3$ for $N_h^1 \leq \alpha \leq N_h^1$ and $N_h^2 \leq \alpha \leq N_h^3$. The horizontal spacing is $\Delta\eta$, uniform across subdomains. The position of grid points along the ξ -axis is given by eq. (44a), while the position along the η -axis is

$$\eta_\beta = \left(\beta - \frac{1}{2}\right) \Delta\eta. \quad (44b)$$

Indices j, k will be restricted to integer values. In the light of the linear stability analysis we will perform in part II, we keep time as a continuous variable, thus $h_j = h(\xi_j, \tau)$, $T_{jk} = T(\xi_j, \eta_k, \tau)$, etc. Bed elevation remains a known, differentiable function of x , so $b_{j+1/2} = b((\xi - (\xi_0)_j)[(x_d)_j - (x_u)_j]$, where $((\xi_0)_j, (x_d)_j, (x_u)_j) = (0, x_s, 0)$ for $1 \leq j \leq N_h^1$, $((\xi_0)_j, (x_d)_j, (x_u)_j) = (1, x_t, x_s)$ for $N_h^1 \leq j \leq N_h^1$, and $((\xi_0)_j, (x_d)_j, (x_u)_j) = (2, x_g, x_t)$ for $N_h^2 \leq \alpha \leq N_h^3$.

4.2.1 Ice thickness evolution

For $1 \leq j \leq N_h^1 + N_h^2 + N_h^3$, equation (39a) is discretised as

$$\frac{\partial}{\partial \tau} [(x_d)_j - (x_u)_j] h_j + \frac{(q_e)_{j+1/2} - (q_e)_{j-1/2}}{\Delta\xi_j^i} - [(x_d)_j - (x_u)_j] \dot{b} = 0. \quad (45a)$$

The effective mass flux, as well as the effective horizontal velocity, are split in the sum of a deformational, a sliding, and an apparent component as

$$(q_e)_{j+1/2} = (q_d)_{j+1/2} + (q_b)_{j+1/2} + (q_a)_{j+1/2}, \quad (u_e)_{j+1/2,k} = (u_d)_{j+1/2,k} + (u_b)_{j+1/2} + (u_a)_{j+1/2}, \quad (45b)$$

where the latter represents the mass flux resulting from motion of the boundaries in the stretched coordinate system. As for the flux, we discretize the deformational component with a second-order centered scheme in the vertical, while we use a first-order upwind scheme to stabilize the advective

part,

$$(q_d)_{j+1/2} = \frac{\Delta\eta}{2} h_{j+1/2} \sum_{k=1}^{k=N^v} [(u_d)_{j+1/2,k+1/2} - (u_d)_{j+1/2,k-1/2}], \quad (45c)$$

$$(q_b)_{j+1/2} = (u_b)_{j+1/2} h_j, \quad (45d)$$

$$(q_a)_{j+1/2} = (u_a)_{j+1/2} h_j, \quad (45e)$$

where $h_{j+1/2}$ is computed with a centered scheme that accounts for variable cell length,

$$h_{j+1/2} = \frac{h_j [(x_d)_{j+1} - (x_u)_{j+1}] \Delta\xi_{j+1} + h_{j+1} [(x_d)_j - (x_u)_j] \Delta\xi_j}{[(x_d)_{j+1} - (x_u)_{j+1}] \Delta\xi_{j+1} + [(x_d)_j - (x_u)_j] \Delta\xi_j}. \quad (45f)$$

For the upwind scheme used for the advective component of the mass flux we have prescribed the direction of advection to be in the positive ξ direction. We note that this is necessarily the case for the steady state and linear stability computations we are interested in, but in an unsteady problem the direction of advection should be allowed to change depending on the sign of u_e .

We now look at the discretization of the horizontal velocity. The deformational velocity is discretized with a second-order centered scheme that accounts for variable cell size

$$(u_d)_{j+1/2,\alpha} = -\frac{(h_{j+1/2})^2}{2} [1 - (1 - \eta_\alpha)^2] \left(\left. \frac{db}{dx} \right|_{j+1/2} + \frac{2(h_{j+1} - h_j)}{[(x_d)_{j+1} - (x_u)_{j+1}] \Delta\xi_{j+1} + [(x_d)_j - (x_u)_j] \Delta\xi_j} \right), \quad (45g)$$

while for the sliding velocity we have

$$(u_b)_{j+1/2} = 0 \quad \text{for } 1 \leq j \leq N_h^1, \quad (45h)$$

$$(u_b)_{j+1/2} = \frac{1}{\alpha(\tau_b)_{j+1/2}} (Q_{j+1/2} - \nu) \quad \text{for } N_h^1 < j \leq N_h^2, \quad (45i)$$

$$(u_b)_{j+1/2} = \frac{1}{\gamma} (\tau_b)_{j+1/2} \quad \text{for } N_h^2 < j \leq N_h^3, \quad (45j)$$

with

$$(\tau_{xz})_{j+1/2,\alpha} = -h_{j+1/2} (1 - \eta_\alpha) \left(\left. \frac{db}{dx} \right|_{j+1/2} + \frac{2(h_{j+1} - h_j)}{[(x_d)_{j+1} - (x_u)_{j+1}] \Delta\xi_{j+1} + [(x_d)_j - (x_u)_j] \Delta\xi_j} \right), \quad (45k)$$

so that $(\tau_b)_{j+1/2} = (\tau_{xz})_{j+1/2,\alpha=1/2}$.

The sliding velocity in the subtemperate region, $N_h^1 \leq j \leq N_h^2$, requires the basal heat flux $Q_{j+1/2}$. Considering the time-like nature of the horizontal direction for the heat equation, and taking advantage of the Dirichlet condition at the bed (40e), we implement the first-order upwind scheme

$$Q_{j+1/2} = -\frac{1}{h_{j+1/2}} \frac{2}{\Delta\eta} T_{j+1/2,1}, \quad T_{j+1/2,k} = T_j, \quad (45l)$$

where once again we have prescribed that advection is in the positive ξ direction.

Finally, the discrete apparent velocity reads

$$(u_a)_{j+1/2} = [\xi_{j+1/2} - ((\xi_0)_j + 1)] \frac{\partial(x_u)_j}{\partial t} - (\xi_{j+1/2} - (\xi_0)_j) \frac{\partial(x_d)_j}{\partial t}. \quad (45m)$$

We now consider boundary conditions. For $j = 1$ eq. (45a) involves the grid point $\alpha = j - 1/2 = 1/2$, located at $\xi = 0$. Here the symmetry condition at the divide, eq. (39j), holds, thus we put

$$(q_e)_{1/2} = q_{1/2} = 0. \quad (45n)$$

For $j = N_h^1 + N_h^2 + N_h^3$, we have the grid point $\alpha = j + 1/2 = N_h^1 + N_h^2 + N_h^3 + 1/2$ located on the grounding line at $\xi = 3$. We compute ice thickness on the grounding line by linearly extrapolating onto the boundary from the two nearest h -grid points,

$$h_{N_h^1+N_h^2+N_h^3+1/2} = \frac{3h_{N_h^1+N_h^2+N_h^3} - h_{N_h^1+N_h^2+N_h^3-1}}{2}, \quad (45o)$$

while eq. (39m) demands

$$(q_d)_{N_h^1+N_h^2+N_h^3+1/2} + (q_b)_{N_h^1+N_h^2+N_h^3+1/2} = Q_g(h_{N_h^1+N_h^2+N_h^3+1/2}), \quad (45p)$$

where the right hand side is known. We are now going to show that the latter equation effectively constrains the sliding velocity at the grounding line. In fact, we can fix $(q_d)_{N_h^1+N_h^2+N_h^3+1/2}$ with the aid of eq. (45g) and using a one-sided approximation for surface slope, which provides h at the fictitious grid point $N_h^1 + N_h^2 + N_h^3 + 1$

$$h_{N_h^1+N_h^2+N_h^3+1} = 2h_{N_h^1+N_h^2+N_h^3} - h_{N_h^1+N_h^2+N_h^3-1}. \quad (45q)$$

Then, with q_b given by (45d) and with the help of (45o), it is clear that the only unknown in eq. (45p) is $(u_b)_{N_h^1+N_h^2+N_h^3+1/2}$, which we fix in such a way to balance the prescribed grounding line flux. This approach allows us to keep consistency between prescribed grounding line flux and sliding and deformational components of the mass flux, yet avoiding to use Q_g to back out the stress at the grounding line, which would be physically meaningless.

Lastly, at the junctions between subdomains, $\alpha = N_h^1 + 1/2$, $\alpha = N_h^1 + N_h^2 + 1/2$, the finite volume scheme ensures that q is conserved automatically, while the centered scheme for h effectively ensures continuity of the ice thickness.

4.2.2 Temperature evolution

For $1 \leq j \leq N_h^1 + N_h^2 + N_h^3$ and $1 \leq k \leq N_v$, equation (40a) is discretized as

$$\begin{aligned} \frac{\partial}{\partial \tau} [(x_d)_j - (x_u)_j] h_j T_{j,k} &+ 2 \frac{(u_e)_{j+1/2,k} h_{j+1/2} T_{j,k} - (u_e)_{j-1/2,k} h_{j-1/2} T_{j-1,k}}{[(x_d)_{j+1} - (x_u)_{j+1}] \Delta \xi_{j+1} + [(x_d)_j - (x_u)_j] \Delta \xi_j} + \\ &\frac{[(x_d)_j - (x_u)_j]}{\Delta \eta} \left[(w_e)_{j,k+1/2} \frac{T_{j,k+1} + T_{j,k}}{2} - (w_e)_{j,k-1/2} \frac{T_{j,k} + T_{j,k-1}}{2} \right] + \\ &\frac{[(x_d)_j - (x_u)_j] [T_{j,k-1} - 2T_{j,k} + T_{j,k+1}]}{Pe h_j \Delta \eta^2} - \frac{\alpha}{Pe} [(x_d)_j - (x_u)_j] S_{j,k} = 0. \end{aligned} \quad (46a)$$

where we have adopted the first-order upwind scheme (45l₂) for horizontal heat fluxes, and we have discretised vertical fluxes with a second-order centered scheme. The horizontal effective velocity is given by (45b) and subsequent closure relations, while an expression for $(w_e)_{j,\beta}$ follows from the discrete version of (42a) with (42b).

Using a second-order centered scheme for the vertical velocity we get

$$\begin{aligned} (w_e)_{j,k+1/2} &= k \Delta \eta \left[\frac{(q_d)_{j+1/2} - (q_d)_{j-1/2}}{[(x_d)_j - (x_u)_j] \Delta \xi_j} \right] - k \dot{b} \Delta \eta - \\ &\Delta \eta \frac{h_{j+1/2} \sum_{\beta=1}^k [(u_d)_{j+1/2,\alpha}] - h_{j-1/2} \sum_{\beta=1}^k [(u_d)_{j-1/2,\alpha}]}{[(x_d)_j - (x_u)_j] \Delta \xi_j}. \end{aligned} \quad (46b)$$

Recalling that $\Delta\eta = N_v^{-1}$, and with $(q_d)_{j+1/2}$ given by (45c), it is straightforward to show that at the surface the effective velocity balances the accumulation term, $(w_e)_{j,N_v+1/2} = -\dot{b}$, meaning that the vertical velocity is effectively mass-conserving.

The discretisation of the heating term $S_{j,k}$ is chosen to ensure global conservation of energy, that is, the volumetric heating integrated over the domain balances the rate of loss of potential energy in discrete terms. We have

$$S_{j,k} = \frac{S_{j+1/2,k} + S_{j-1/2,k}}{2}, \quad (46c)$$

with

$$S_{j+1/2,k} = \left(\frac{(u_d)_{j+1/2,k+1/2} - (u_d)_{j+1/2,k-1/2}}{\Delta\eta} \right) \left(\frac{(\tau_{xz})_{j+1/2,k+1/2} + (\tau_{xz})_{j+1/2,k-1/2}}{2} \right) \quad (46d)$$

with $(\tau_{x,z})_{j+1/2,\alpha}$ and $(u_d)_{j+1/2,\alpha}$ given by eqs. (45g), (45k), respectively. On domain boundaries, respectively for $\alpha = j - 1/2 = 1/2$ and $\alpha = j + 1/2 = N_h^1 + N_h^2 + N_h^3 + 1/2$ we set

$$S_{1/2,k} = 0, \quad S_{N_h^1+N_h^2+N_h^3+1/2,k} = S_{N_h^1+N_h^2+N_h^3,k}, \quad (46e)$$

where the former follows from the symmetry of the divide, while the latter uses an upwind scheme for the computation of the heating term at the grounding line in order to avoid using Q_g to back out the shear stress on the grounding line itself.

Next we consider boundary conditions. For $j = 1$ eq. (46a) involves the grid point $\alpha = j - 1/2 = 1/2$, which with the upwind scheme (45l₂) demands T at the fictitious grid point $j = 0$. By symmetry across the divide, we have

$$T_{0,k} = T_{1,k}, \quad (u_e)_{1/2,k} = 0, \quad (46f)$$

which ensures that the horizontal heat flux vanish there, while at the junctions between subdomains the finite volume scheme ensures that temperature remains continuous.

For $k = N_v$, we require temperature at the fictitious grid point $\beta = j = N_v + 1$. In order to satisfy the Dirichlet condition (40c) on the domain boundary, $j = N_v + 1/2$, by symmetry we put

$$T_{j,N_v+1} = -2 - T_{j,N_v}. \quad (46g)$$

Lastly, at the bed, we need to specify temperature at the fictitious grid points $\beta = j = 0$. Here we need to satisfy the Neumann condition (40d) for $1 \leq j \leq N_h^1$, while we have the Dirichlet condition (40e) for $j \geq N_h^1$. Thus we put

$$T_{j,0} = T_{j,1} + h_j \nu \Delta\eta \quad \text{for } 1 \leq j \leq N_h^1, \quad T_{j,0} = -T_{j,1} \quad \text{for } j \geq N_h^1. \quad (46h)$$

4.2.3 Sub-domain boundaries

Lastly, we need to determine the position of subdomain boundaries. From the conditions (43) and the flotation condition (39l) we have

$$-\frac{1}{h_{j+1/2}} \frac{T_{j+1/2,1}}{\Delta\eta} = \nu \quad \text{for } j = N_h^1, \quad (47a)$$

$$\frac{1}{h_{j+1/2}} \frac{T_{j+1/2,1}}{\Delta\eta} + \nu + \alpha(\tau_b)_{j+1/2}(u_b)_{j+1/2} = 0 \quad \text{for } j = N_h^1 + N_h^2, \quad (47b)$$

$$h_{j+1/2} = -\frac{\rho}{\rho_w} b_{j+1/2} \quad \text{for } j = N_h^1 + N_h^2 + N_h^3, \quad (47c)$$

where we use the upwind scheme (45l₂) for $T_{j+1/2,1}$, and $h_{N_h^1+N_h^2+N_h^3+1/2}$ is obtained by linear extrapolation onto the boundary as described by eq. (45o).

4.3 Numerical solution of the steady state problem

To compute steady state solutions, we start with setting time derivatives to zero in eqs. (45a, 46a). Then, for a given set of locations for the free boundaries x_s , x_t and x_g as well as a given ice thickness h_0 at the centre of the ice sheet, ice thickness, temperature and ice velocity can be solved for sequentially, one column of grid cells at a time.

In steady state, ice flux is known at every horizontal cell boundary from the integral of surface mass balance,

$$(q_d)_{j+1/2} + (q_b)_{j+1/2} = [(x_d)_j - (x_u)_j] \dot{b} \Delta \xi_j^i + (q_d)_{j-1/2} + (q_b)_{j-1/2} \quad (48a)$$

with symmetry at the divide demanding that

$$(q_d)_{j-1/2} = (q_b)_{j-1/2} = 0 \quad \text{for } j = 1. \quad (48b)$$

With basal heat flux at the cell boundary $j + 1/2$ set equal to its upstream cell centre value (see eq. (45l)), the known ice flux corresponds to a unique velocity field and, through the dependence of the velocity field on surface slope (either through 45g or through 45i, 45j, and 45k), we can compute ice thickness at the next cell centre downstream, $j + 1$. Depending on the subdomain, the computation of h_{j+1} may or may not decouple from the computation of temperature: in the cold and temperate subdomains the two are fully decoupled, so we solve eq. (45a) at prescribed along-flow location j with a backward Euler step in the horizontal coordinate to find h_{j+1} , and then solve the linear temperature problem (46a) for $T_{j,k}$ with prescribed velocity field. In the subtemperate region mass and energy conservation are coupled through the sliding law, so we solve the fully coupled problem with a backward Euler step in the horizontal coordinate to find h_{j+1} and $T_{j,k}$.

For a given guess for (h_0, x_c, x_s, x_g) , we can therefore compute the residual of the continuity conditions (47a-47b) at x_s , x_t , and in the flotation and flux condition at x_g , eqs. (47c, 45p). Solving the steady state problem amounts to finding the appropriate roots that reduce all four residuals to zero. We do so by means of a bisection algorithm, with accuracy set at 10^{-4} .

4.4 A discontinuous acceleration at the subtemperate - temperate boundary

One peculiar feature of the boundary conditions (37) is that the sliding velocity remains continuous at sub-domain boundaries, $x = x_s, x_t$. However, the acceleration might be discontinuous across the transition points, leading to streamlines that are continuous but not differentiable. In this section we illustrate that this is actually the case in the context of a standard shallow ice model, and derive constraints for the sign of the jump in gradients of sliding velocity and basal heat flux normal to the subtemperate-temperate boundary.

Let us consider the ice sheet scale model presented in §(2.1) and updated with basal boundary conditions (37) and continuity statements at subdomain boundaries (37d). With the mass flux defined as

$$q = \frac{h^2}{3} \tau_b + u_b h, \quad (49a)$$

continuity of mass flux and thickness imply that the basal shear stress and strain heating are also continuous,

$$[\tau_b]_-^+ = [a]_-^+ = 0, \quad (49b)$$

with the former in turn implying

$$\left[\frac{\partial h}{\partial x} \right]_-^+ = 0. \quad (49c)$$

Equipped with these continuity statements, we use the large scale mass conservation, eq. (7c) to derive a relationship between $\partial u_b / \partial x$ on either sides of the boundary. Given that the accumulation rate \dot{b} is continuous at $x = x_t$, it follows from mass conservation that

$$\left[\frac{\partial q}{\partial x} \right]_-^+ = 0 \quad (49d)$$

in a steady state. Using the definition of the flux (49a) and the continuity statements (37d, 49c) we can rewrite the latter expression as

$$\left[\frac{\partial q}{\partial x} \right]_-^+ = \frac{h^2}{3} \left[\frac{\partial \tau_b}{\partial x} \right]_-^+ + h \left[\frac{\partial u_b}{\partial x} \right]_-^+ = 0. \quad (49e)$$

Direct differentiation of the sliding law

$$u_b = \begin{cases} \gamma^{-1} \tau_b & \text{on } x > x_t \\ \frac{Q - \nu}{\alpha \tau_b} & \text{on } x < x_t \end{cases} \quad (49f)$$

where $Q = -\partial T / \partial z|_{z=b}$ is the basal heat flux then yields an expression for $\partial \tau_b / \partial x$ in terms of derivatives of the heat flux and the sliding velocity,

$$\left. \frac{\partial \tau_b}{\partial x} \right|^+ = \left. \frac{\tau_b}{u_b} \frac{\partial u_b}{\partial x} \right|^+, \quad (49g)$$

$$\left. \frac{\partial \tau_b}{\partial x} \right|^- = \left. \frac{1}{\alpha u_b} \frac{\partial Q}{\partial x} \right|^- - \left. \frac{\tau_b}{u_b} \frac{\partial u_b}{\partial x} \right|^-, \quad (49h)$$

which substituted into (49e) allows us to derive a relationship between the gradient of the sliding velocity on either sides of the transition and the gradient of the subtemperate heat flux,

$$\left(1 + \frac{h}{3} \frac{\tau_b}{u_b} \right) \left. \frac{\partial u_b}{\partial x} \right|^+ = \left(1 - \frac{h}{3} \frac{\tau_b}{u_b} \right) \left. \frac{\partial u_b}{\partial x} \right|^- + \frac{h}{3\alpha u_b} \left. \frac{\partial Q}{\partial x} \right|^- . \quad (49i)$$

In order to close the problem, we need a constraint on the sign of the velocity gradients, as well as a relationship between the sliding velocity and the gradient of the basal heat flux. The former is provided by the requirement that the bed does not freeze on the temperate side,

$$-Q + \nu + \alpha \tau_b u_b \geq 0 \quad \text{on } x > x_t. \quad (49j)$$

Taylor-expanding about $x = x_t$, and recalling that the equality must hold at the transition proper, we find

$$\alpha \left(\tau_b \left. \frac{\partial u_b}{\partial x} \right|^+ + u_b \left. \frac{\partial \tau_b}{\partial x} \right|^+ \right) \geq \left. \frac{\partial Q}{\partial x} \right|^+. \quad (49k)$$

Then, in order to find a relationship between velocity and flux gradients, we extend the derivation of the Q -equation (§3b of the main paper) to the case of $Pe \sim O(1)$. Following the derivation in the main text, but starting with eq. (9a), we find

$$u_b \frac{\partial Q}{\partial x} - Q \frac{\partial u_b}{\partial x} - \frac{1}{Pe} \frac{\partial^2 Q}{\partial z^2} = \frac{\alpha}{Pe} \left. \frac{\partial a}{\partial z} \right|_{z=b}, \quad (49l)$$

which holds in both the subtemperate and temperate subdomains at the ice sheet scale. Taking the difference across the boundary, we have

$$u_b \left[\frac{\partial Q}{\partial x} \right]_-^+ - Q \left[\frac{\partial u_b}{\partial x} \right]_-^+ = \frac{1}{Pe} \left[\frac{\partial^2 Q}{\partial z^2} \right]_-^+ + \frac{\alpha}{Pe} \left[\frac{\partial a}{\partial z} \right]_-^+, \quad (49m)$$

where the two rhs terms vanish as a result of the continuity statements (37d, 49b). We are therefore left with the desired relationship between flux and sliding velocity gradients at the transition,

$$u_b \left[\frac{\partial Q}{\partial x} \right]_-^+ - Q \left[\frac{\partial u_b}{\partial x} \right]_-^+ = 0. \quad (49n)$$

Finally, we find a constraint on the sign of $[\partial u_b / \partial x]_-^+$ by combining (49k) with (49i), and making use of (49n), (49g) and (49f), leading to

$$\left(\frac{3\alpha u_b}{h} + \frac{\nu}{u_b} \right) \left[\frac{\partial u_b}{\partial x} \right]_-^+ \leq 0. \quad (49o)$$

The term in brackets is strictly positive, therefore $[\partial u_b / \partial x]_-^+$ can either be negative, or vanish. The equality holds at the transition point, but we expect the basal energy budget to turn positive as we move away from the transition point into the temperate subdomain. Therefore we conclude that $[\partial u_b / \partial x]_-^+$ has to be negative, and so is $[\partial Q / \partial x]_-^+$ from (49n).

5 The length of the subtemperate region with $Pe = 0$

5.1 On Fowler's (2001) argument about the impossibility of a hard switch

In this section we revisit the argument in Fowler [9] and Fowler and Larson [3] on the necessity of an extended subtemperate region, and demonstrate that it does not automatically apply to the case of a finite Péclet number.

Let us consider a frozen-temperate transition that involves an extended region of subtemperate sliding for $x \in [x_s, x_t]$, such that at the bed we have

$$-Q + \nu + \alpha \tau_b u_b = 0, \quad u_b = F(T/\delta, \tau_b) \quad \text{on} \quad z = b, \quad (50)$$

and the sliding velocity is such that $u_b(x_s) = 0$ and $u_b(x_t) = \gamma^{-1} \tau_b$, with $u_b < \gamma^{-1} \tau_b$ for $x < x_t$.

Then, assuming that the shallow ice model of §2.1 holds for ice mechanics, and also assuming a strongly diffusive temperature field, $Pe = 0$, the heat transport problem for the ice reduces to

$$-\frac{\partial^2 T}{\partial z^2} = \alpha \left(\frac{\partial u}{\partial z} \right)^2 \quad \text{for} \quad b < z < s, \quad (51a)$$

with prescribed surface temperature

$$T = T_S(x) \quad \text{on} \quad z = s, \quad (51b)$$

and the basal energy budget condition eq. (50₁) at the bed.

We are now going to illustrate that, under these conditions, the temperature-dependent sliding law $u_b = f(T, \tau_b)$ can be rewritten as $u_b = g(T_s, q)$, where $q = \int_b^s u \, dz$ is the ice flux. As far as the heat equation is concerned, integrating eq. (51a) once on $b < z < s$ and using the shallow ice solution (7a) yields

$$-\frac{\partial T}{\partial z}\bigg|_b^s = \alpha |\nabla s|^2 \frac{h^3}{3}; \quad (52)$$

substituting then the heat flux $Q = -\partial T / \partial z|_{z=b}$ from the basal energy budget (50₁) gives an expression for the heat flux at the surface

$$-\frac{\partial T}{\partial z} = \nu + \alpha |\nabla s| q \quad \text{on} \quad z = s. \quad (53)$$

Equipped with this latter expression, as well as with the Dirichlet condition (51b), we can now see the diffusion problem (51a) as a well-posed initial value problem that provides basal temperature as a function of a prescribed distribution of surface temperature, $T_s(x)$, and automatically satisfies the constraint of a basal energy budget in balance.

Now, taking the limit of $\delta \rightarrow 0$, basal temperature is prescribed in the subtemperate region and equal to the melting point. Then, for a prescribed mass flux, and with fixed temperature at the bed, the initial value problem for T effectively determines the ice thickness and the basal shear stress as functions of T_s . Knowing the ice thickness, the sliding velocity can be backed out from the basal energy budget, and is therefore also a function of T_s and q , as previously advertised. Lastly, the mass flux is the solution to the global mass conservation, while once again the sliding law constrains the first order correction to basal temperature.

From here, Fowler [9] uses a continuity argument to demonstrate that the sliding velocity cannot be discontinuous, and therefore the boundaries of the subtemperate region x_s and x_t cannot collapse onto each other as δ vanishes. The argument goes as follows: by construction, the sliding velocity $u_b = g(T_s, q)$ changes of $O(1)$ across the subtemperate region, and does so continuously because T_s and q are continuous functions of x . If taking the limit of $\delta \rightarrow 0$ caused the subtemperate region to become infinitesimal, then this would imply a discontinuity in u_b , which is not possible given that T_s and q are continuous functions of x .

It is now clear why the argument that allowed us to formulate the heat equation as an initial value problem in z cannot be extended to the case of a finite Péclet number: in fact, when $Pe > 0$ the heat equation becomes a parabolic problem with the horizontal coordinate acting in a time-like fashion (as opposed to the second order ordinary differential equation problem for $Pe = 0$, which Fowler [9] effectively tackles by a shooting method). Then, the depth-integration described above requires us to impose two boundary conditions on a space-like boundary for a parabolic PDE, which is an ill-posed procedure. Fowler's argument therefore does not demonstrate that the subtemperate region must be comparable in length with the ice sheet scale when $Pe \neq 0$.

5.2 A constraint from energy conservation

In this section we are going to take a different, more physically based approach to the problem discussed by Fowler [9], which will allow us to highlight the physical paradox hidden behind the notion of a hard switch in the $Pe = 0$ case. The key insight is that, at constant mass flux, ice flow by shearing only dissipates more potential energy — and therefore produces more heat — than ice flow by sliding *and* shearing. As a result, even if the melting point is reached, the decrease in energy dissipation caused by sliding onset leads to refreezing immediately thereafter.

The ingredients we require to demonstrate that this is true are (i) the solution to the heat equation in the ice for $Pe = 0$ in the two cases of a frozen bed and of a prescribed melting point temperature at the base. We will see shortly that the temperature T in the case of $Pe = 0$ can be written in closed form as a function of ice thickness h and surface slope $|\partial s/\partial x|$. (ii) The definition of the mass flux q for the two cases of flow by shearing only, and shearing and sliding combined. Note that q also is a function of h and $|\partial s/\partial x|$. (iii) The inequality constraints demanding that bed temperature is below freezing on the cold side, and that the melt rate remains positive on the temperate side. Once again, these can be written in closed form only by virtue of having taken $Pe = 0$.

Equipped with these ingredients, we will show that if the ice thickness is to be conserved at the transition point, $x = x_{onset}$, as it must, then the inequality constraints can be satisfied only if the ice flux changes discontinuously across the transition, which violates mass conservation. Our conclusion about the potential energy dissipation rate follows straightforwardly.

The derivation goes as follows. Given a standard shallow ice approximation for the velocity field (7a), and assuming without loss of generality that $b = 0$, the solution of the diffusion-only problem (9) with $Pe = 0$ reads

$$T = \begin{cases} \frac{\alpha}{3} \left| \frac{\partial h}{\partial x} \right|^2 \left[-\frac{(h-z)^4}{4} - zh^3 + h^4 \right] + \nu(h-z) - 1 & \text{for } 0 < z < h, \\ \frac{\alpha}{4} \left| \frac{\partial h}{\partial x} \right|^2 h^4 + \nu(h-z) - 1 & \text{for } -\infty < z < 0, \end{cases} \quad (54a)$$

while for temperate bed we have

$$T = \begin{cases} \frac{\alpha}{12} \left| \frac{\partial h}{\partial x} \right|^2 [-(h-z)^4 - zh^3 + h^4] - \frac{z}{h} & \text{for } 0 < z < h, \\ -\nu z & \text{for } -\infty < z < 0, \end{cases} \quad (54b)$$

which substituted into the inequality constraints yield

$$\text{either} \quad -1 + \nu h + \alpha \left| \frac{\partial h}{\partial x} \right|^2 \left(\frac{h^4}{4} + \frac{1}{\gamma} h^3 \right) \geq 0 \quad \text{if} \quad T = 0 \quad \text{on} \quad z = 0, \quad (54c)$$

$$\text{or} \quad -1 + \nu h + \frac{\alpha}{4} \left| \frac{\partial h}{\partial x} \right|^2 h^4 < 0 \quad \text{if} \quad T < 0 \quad \text{on} \quad z = 0. \quad (54d)$$

Let us recall that we intend to turn the inequality constraints (54c) into constraints for the mass flux on either sides of the transition. To do so, let us denote the cold, upstream region with \cdot^- and the warm downstream region with \cdot^+ , and recall that the respective mass fluxes are given by

$$q^- = \frac{1}{3} h^3 \left| \frac{\partial h}{\partial x} \right|^- , \quad (54e)$$

$$q^+ = \left(\frac{1}{3} h^3 + \frac{1}{\gamma} h^2 \right) \left| \frac{\partial h}{\partial x} \right|^+ . \quad (54f)$$

Then the inequality constraints (54c) can be reformulated in terms of ice flux as

$$q^2 < (q^-)^2 := \frac{4(1 - h\nu)(h^3/3)^2}{\alpha h^4}, \quad (54g)$$

$$q^2 \geq (q^+)^2 := \frac{4(1 - \nu h)(h^3/3 + h^2/\gamma)^2}{\alpha(h^4 + 4h^3/\gamma)}. \quad (54h)$$

In order to conserve mass across the transition point while at the same time satisfying the inequality constraints, then the upstream and downstream flux must satisfy $(q^+)^2 < (q^-)^2$, or equivalently

$$\left(\frac{q^-}{q^+}\right)^2 := \frac{(1+3\Gamma)^2}{1+4\Gamma} < 1, \quad \text{with } \Gamma = (\gamma h)^{-1}. \quad (54i)$$

It is straightforward to show that the latter inequality cannot be satisfied. In fact, we have $(q^-/q^+)^2 = 1$ for $\Gamma = 0$ and

$$\frac{d}{d\Gamma}(1+3\Gamma)^2 > \frac{d}{d\Gamma}(1+4\Gamma), \quad (54j)$$

so we can conclude that $(q^-/q^+)^2 > 1$; in other words, mass conservation and the inequality constraints regulating the thermal state of the bed cannot be satisfied simultaneously, meaning that an abrupt transition is energetically impossible.

The physical interpretation of our result is related to energy dissipation. Total dissipation in the flow corresponds to the rate of loss of potential energy, $q|\partial s/\partial x|$. At constant ice thickness and mass flux, as is the case at the transition, surface slope is smaller in the warm-bedded region than it is in the cold one,

$$|\partial h/\partial x|^+ := q/(1/3h^3 + h^2/\gamma) < |\partial h/\partial x|^- := q/(1/3h^3), \quad (55)$$

meaning that the cold branch of the solution dissipates more heat than the temperate branch. This is because dissipation by strain heating, $(s-z)|\partial s/\partial x|^2$, is smaller on the temperate side as a result of reduced surface slope, and frictional heating at the bed is not large enough to offset larger dissipation on the cold side. As a result of this disparity in dissipation rate, a warm-bedded region can only exist for values of the mass flux larger than those at which the cold-bedded region persists.

References

- [1] J. Weertman. On the sliding of glaciers. *J. Glaciol.*, 3:33–38, 1957.
- [2] A.C. Fowler. A theoretical treatment of the sliding of glaciers in the absence of cavitation. *Philos. Trans. R. Soc. Lond. A*, 298:637–685, 1981.
- [3] A.C. Fowler and D.A. Larson. On the flow of polythermal glaciers. i. Model and preliminary analysis. *Proc. R. Soc. Lond. A*, 363:217–242, 1978.
- [4] L.W. Morland and I.R. Johnson. The steady motion of ice sheets. *J. Glaciol.*, 25:229–246, 1980.
- [5] M. Haseloff, C. Schoof, and O. Gagliardini. A boundary layer model for ice stream margins. *J. Fluid Mech.*, 781:353–387, 2015.
- [6] M. Haseloff, C. Schoof, and O. Gagliardini. The role of subtemperate slip in thermally driven ice stream margin migration. *The Cryosphere*, 12(8):2545–2568, 2018.
- [7] V. Barcilon and D. R. MacAyeal. Steady flow of a viscous ice stream across a no-slip free-slip transition at the bed. *J. Glaciol.*, 39(131):167–185, 1993.
- [8] C. Schoof. Thermally driven migration of ice-stream shear margins. *J. Fluid. Mech.*, 712: 552–578, 2012.

- [9] A.C. Fowler. Modelling the flow of glaciers and ice sheets. In *Continuum Mechanics and Applications in Geophysics and the Environment*, pages 201–221. Springer, Berlin, 2001.
- [10] G. K. Batchelor. *An Introduction to Fluid Dynamics*. Cambridge University Press, 2000.
- [11] C. Schoof. Marine ice sheet dynamics. Part 2. A Stokes flow contact problem. *J. Fluid Mech.*, 679:122–155, 2011.